Sandstone petrography and geochemistry of the Nayband Formation (Upper Triassic, Central Iran): Implications for sediment provenance and tectonic setting

Asghar ETESAMPOUR[1)], Asadollah MAHBOUBI[1)*)], Reza MOUSSAVI-HARAMI[1)], Nasser ARZANI[2)] & Mohammad Ali SALEHI[3)]

[1)] Department of Geology, Faculty of Sciences, Ferdowsi University of Mashhad, Mashhad, Iran;

[2)] Department of Geology, Payame Noor University of Isfahan, Isfahan, Iran;

[3)] Department of Geology, Faculty of Sciences, University of Isfahan, Isfahan, Iran;

[*)] Corresponding author: mahboubi@um.ac.ir

Abstract

The Upper Triassic (Norian–Rhaetian) Nayband Formation is situated at the southwestern margin of Central East Iranian Microcontinent and records Eo-Cimmerian events. The formation is composed of mixed carbonate-siliciclastic deposits. This study presents information on the tectonic reconstruction and palaeoclimate of the southwestern margin of Central East Iranian Microcontinent during the Late Triassic. Petrography and modal analyses of sandstones show a variety of quartz-rich petrofacies including subarkose, lithic arkose, sublitharenite, feldspathic litharenite and litharenite. The combined modal analysis and geochemical results of major and trace elements of the sandstone samples represents mixed sedimentary, intermediate, felsic igneous rocks and moderate- to high-grade metamorphic provenance areas. The major elements and modal analyses of the Nayband Formation sandstone samples suggest an active continental margin tectonic settings. The palaeoclimatic conditions were sub-humid to humid with relatively low to moderate weathering in the source area which is in agreement with the palaeogeography and palaeotectonic history of southwestern margin of Central East Iranian Microcontinent during the Late Triassic.

1. Introduction

The composition of siliciclastic rocks is controlled by various factors including transportation processes, geology, tectonic and palaeoclimate of the source area (McLennan et al., 1993; Arribas et al., 2007; Zimmermann and Spalletti, 2009; Adhikari and Wagreich, 2011; Ghazi and Mountney, 2011; Nehyba et al., 2012; Garzanti et al., 2013; Salehi et al., 2014, 2018a; Nehyba and Roetzel, 2015; Fathy et al., 2018; Iqbal et al., 2019). It is possible to determine the composition of the source area in the siliciclastic sediments using the results of geochemical analysis data (e.g. Roser and Korsch, 1988; Armstrong-Altrin et al., 2012). Trace elements are insoluble and usually inactive under superficial conditions, therefore, they are suitable for analysing the source rocks (McLennan et al., 1993; Von-Eyatten et al., 2003). The aim of this study is using modal and geochemical analysis (major and trace elements) to determine the source rock, palaeoweathering, palaeoclimatic conditions, tectonic setting and palaeogeography of siliciclastics of the Nayband Formation in the southwestern margin of Central East Iranian Microcontinent (CEIM) (Fig. 1A). The results provide information on the provenance characteristics of the Upper Triassic deposits in Central Iran in the context of the Eo-Cimmerian Orogeny and the palaeogeographic reconstruction of the Middle-East during Early Mesozoic.

2. Geological setting

The Iran Plate, an element of the Cimmerian Microplate assemblage, was separated from the Arabian Plate following the opening of the Neo-Tethys Ocean in the Late Paleozoic (Wilmsen et al., 2009a). During the Late Triassic, Neo-Tethys subduction started at the southern margin of the Iran Plate (Arvin et al. 2007). The Eo-Cimmerian Orogeny was the result of collision between the Iran Plate and the Turan Plate of Eurasia (e. g. Wilmsen et al., 2009a). This collision is one of the important events in the Early Cimmerian Orogeny (Wilmsen et al., 2009a) and had a crucial role in the deposition of the Middle-Late Triassic successions of the Cimmerian terranes of Iran (Fürsich et al., 2009). The subduction process is inferred to have reduced compressive stress on the interior parts of the Iran Plate, leading to the formation of extensional basins in which a relatively thick succession of shale, sandstone and some carbonates have been deposited on the CEIM (Fürsich et al., 2005; Mannani and Yazdi, 2009; Wilmsen et al., 2009a; Nützel et al., 2010). The extensional phases formed the back-arc basin along the southwestern edge of the Iran Plate (Wilmsen et al., 2009a). This palaeogeographic scenario started with the sedimentation of the Nayband Formation in the southwestern margin of CEIM. The Nayband Formation refers to the Upper Triassic part of this succession (i.e. Shemshak Group) with siliciclastic and

mixed carbonate-siliciclastic deposits. The thickness of these deposits in the type locality (south of Tabas) is 3000 m and includes five members; Gelkan, Bidestan, Howz-e-Sheikh, Howz-e-Khan and Qadir (Fig. 2) (Fürsich et al., 2005). Schäfer et al. (2003) reported that the CEIM was located in the northern margin of the Neo-Tethys at the time of sedimentation of the Nayband Formation. Moreover, earlier studies suggested that the Nayband Formation was deposited on tilted fault blocks of an extensional basin (Fürsich et al., 2005). Although this formation is well developed in the Tabas Block (Fürsich et al., 2005; Bayet-Goll et al., 2018), it is less distinct or absent in the Yazd Block of CEIM (Senowbari-Daryan et al., 2011). The Nayband Formation reappears in the north of Isfahan (southwestern margin of CEIM) where a complete section attains a thickness of more than

one thousand meters and is subdivided into four local informal members (Zahehi, 1973; Seyed-Emami, 2003) (Fig. 2).

3. Methods

A total of 55 samples were collected from three measured stratigraphic sections in the study area. The sandstones samples were named according to the Folk (1980) classification. The modal analysis has been performed on 55 samples of medium-grained sandstone with at least 300 points per sample (Tables 1–3) by the Gazzi-Dickinson method (Ingersoll et al., 1984; Dickinson, 1985). In order to determine the chemical composition of siliciclastic deposits, the bulk of 33 medium-grained, sandstone samples with the least degree of surficial weathering and calcium carbonate contents (less than 5%) were selected
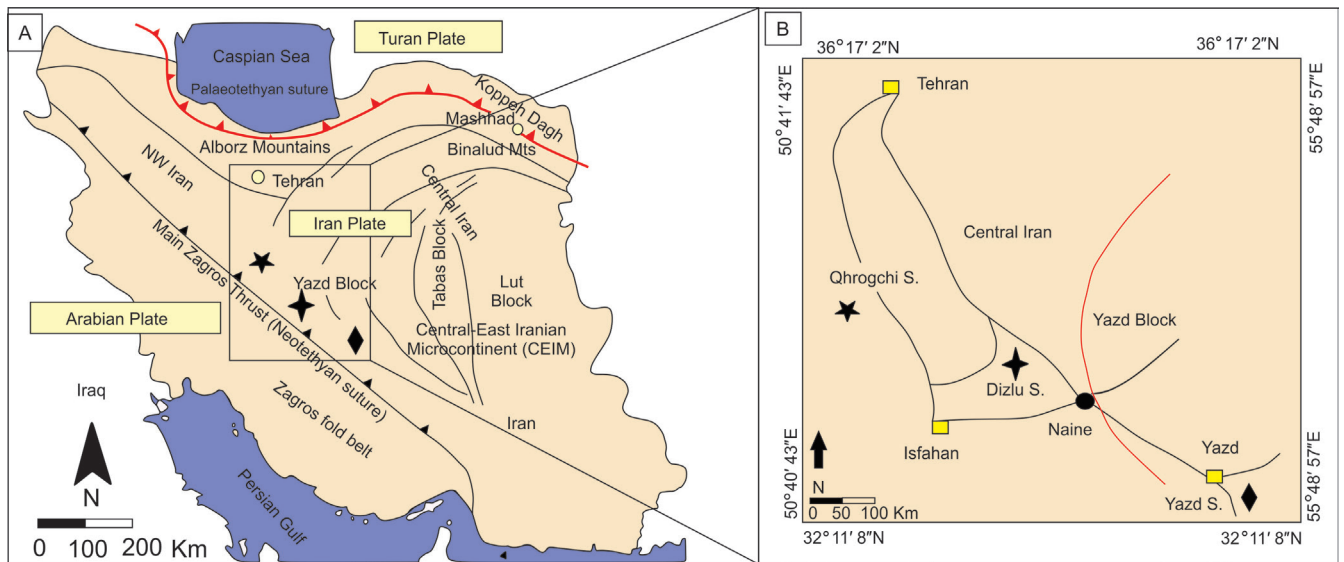

Figure 1: A: Structural and geographic framework of Iran with main sutures, structural units, geographic areas and the location of the studied sections (modified from Wilmsen et al., 2009b), B: Location map showing the access roads to the sections in central Iran.

Figure 2: General stratigraphy of the Upper Triassic rocks of the Nayband area in east-central Iran and comparison with the studied sections in central Iran.

Grain	Description
Qm non	Non-undulose monocrystalline quartz
Qm un	Undulose monocrystalline quartz
Qpq2-3	Qpq2-3 crystal units per grain
Qpq>3	Qpq>3 crystal units per grain
Cht	Chert
Qp	Polycrystalline quartzose (or chalcedonic) Lithic fragments (Qpq+Cht)
Qt	Total quartzose grains (Qm+Qp)
Q	Total (Qm non + Qm un) and Qpq used for Folk (1980) classification (Qm+Qpq)
P	Plagioclase feldspar
K	Porassium feldspar
F	Total feldspar grains (P+K)
SRF, Ls	Sedimentary rock fragments
MRF, Lm	Metamorphic rock fragments
VRF, Lv	Volcanic rock fragments
L	Unstable (siliciclastic) lithic fragments (Lv+Ls+Lm)
Lt	Total siliciclastic lithic fragments (L+Qp)
RF	Total unstable rock fragments and chert used for Folk (1980) classification

Table 1: Framework parameters of detrital modes (modified from Ingersoll and Suczek, 1979).

for analysis of the major elements by Philips-PW1480 XRF instrument and 27 sandstone samples also selected for the trace elements detection by ICP-OES both at Kansaran Binaloud (Mine Material Research Co.), Tehran, Iran (Tables 4–5).

4. Results

4.1 Stratigraphy

In this study, the Nayband Formation was studied in three sections which geographically belong to southwestern margin of CEIM (Fig. 1A, B). In the north of Isfahan the Upper Triassic deposits are overlain with a distinct angular unconformity by Lower Cretaceous deposits, whereas the Jurassic sediments are almost missing completely (Mannani and Yazdi, 2009; Ghasemi-Nejad et al., 2013; Salehi et al., 2018a). Although Lower Jurassic fluvio-deltaic sediments occur in the Tabas Block, the western Lut Block of CEIM, Alborz and adjoining area (Fürsich et al., 2017; Salehi et al., 2018b). The first section is located in 60 km northeast Isfahan in the Dizlu area measured in detail at 33° 04′ 45″ N and 52° 02′ 16″ E with the total thickness of 352 m. It consists of five members (the Gelkan, Bidestan, Howz-e-Sheikh, Howz-e-Khan and Qadir) of Norian to Rhaetian age (Mannani and Yazdi, 2009). In the area, the Nayband Formation rests fault bounded on the Middle Triassic Shotori Formation. The section is composed of three generally classified lithostratigraphic units including lower siliciclastic (the Gelkan Member), mixed carbonate-siliciclastic (the Bidestan, Howz-e-Sheikh and Howz-e-Khan members) and the upper siliciclastic (the Qadir Member) (Figs. 3A, 4). The second section is located 125 km north Isfahan in the Qhrogchi area measured in detail at 33° 36′

55″ N and 50° 59′ 36″ E with the total thickness of 115 m (Gelkan, Bidestan, Howz-e-Sheikh and Howz-e-Khan members). This section passes into recent alluvial deposits. In this section, two lithostratigraphic units can be differentiated including lower siliciclastics (the Gelkan Member) and upper mixed carbonate-siliciclastics (the Bidestan, Howz-e-Sheikh and Howz-e-Khan members) (Figs. 2, 3B, 4). The third section is located in the south Yazd, measured in detail at 31° 48′ 52″ N and 54° 19′ 07″ E with the total thickness of 120 m. It has only one member, the Howz-e-Khan Member (Senowbari-Daryan et al., 2011). The lower part of this section is not exposed and the upper part passes into recent alluvial deposits. This section, similar to the latter section, is composed of two general lithostratigraphic units including lower siliciclastic and upper mixed carbonate-siliciclastic (Figs. 3C, 4).

4.2 Sandstone petrography and modal analysis

Representative photographs of sandstones from the Dizlu, Qhrogchi and Yazd sections are presented in Fig. 5A–F. The sandstone grains are mostly subangular to rounded and their sphericity changes from low to moderate. The sandstones show point, straight, sutured, concavo-convex grain contacts. The sandstones are well to moderately sorted and closer packed. Textural and modal analysis of the sandstone grains indicate sublitharenite (often sub-chertarenite), subarkose, lithic arkose, feldspathic litharenite and litharenite petrofacies (Fig. 6A, B).

The major constituents of these sandstones are quartz, feldspars and rock fragments (sedimentary and metamorphic rock fragments). Among quartz grains, monocrystalline quartz is more frequent than polycrystalline quartz (Qp 2-3 and Qp>3) (Fig. 5A, C). The second component of sandstones is feldspar (Fig. 5 B, D). Plagioclase dominates over K-feldspar. The rock fragments mainly include sedimentary (chert) and metamorphic (schist) (Fig. 5F). The average percentage of the various types of quartz, feldspar and rock fragment is 77, 12 and 11 %, respectively in all identified petrofacies of the Nayband Formation (Table 3).

4.3 Geochemistry

The results of the elemental (major and minor) analysis of studied samples of the Nayband Formation are presented in Tables 4 and 5. The major elements composition is normalized against the upper continental crust (UCC) composition (Taylor and McLennan, 1985) (Fig. 7). The comparison of the data shows that with the exception of SiO_2, MnO and CaO all the other major elements are showing depletion in the sandstones relative to the average values of the UCC. All samples are slightly more depleted in MgO and K_2O relative to UCC. The trace elements are also normalized against the UCC composition (McLennan, 2001) (Fig. 8). The values of all elements are depleted relative to UCC.

Sample No.	section and member		Qm un	Qm nun	Qp2-3	QP>3	Q met	K fel	Pl	Lm	Cht	Acc	HM	cement	Sum
Q1-1			102	148	28	1	9	20	19	10	4	0	5	24	370
Q3-1			47	142	42	14	4	21	11	15	12	2	5	27	342
Q4-1			66	164	18	14	13	7	8	10	5	9	2	26	344
Q5-1			46	180	33	17	0	27	14	18	4	3	10	41	393
Q6-1		Qadir Mb	55	156	20	13	0	31	8	14	8	9	5	25	344
Q8-1			71	142	21	16	1	34	20	18	10	7	2	35	379
Q10-1			99	152	39	39	19	21	15	27	26	1	2	5	483
Q11-1			88	168	24	12	18	21	8	14	9	0	1	17	386
Q12-1			35	167	17	6	5	36	28	26	8	6	5	19	358
Q13-1			38	131	28	9	11	20	17	52	2	5	1	24	338
Q14-1			49	120	32	17	26	43	21	8	10	0	2	8	336
G2-1	Dizlu		95	83	47	19	23	35	15	18	14	1	0	8	360
G3-1			92	109	34	9	16	27	18	6	14	2	3	15	345
G4-1			80	118	46	21	11	23	18	7	12	0	4	9	349
G5-1			95	128	31	19	46	21	25	9	14	0	0	30	418
G5-2			82	118	19	11	37	27	30	5	21	2	12	11	375
G5-3			135	110	23	11	27	25	24	10	11	2	10	45	433
G6-2		Gelkan Mb	136	95	13	6	11	23	25	11	20	1	6	14	361
G7-1			104	115	6	6	13	28	31	10	11	4	0	15	343
G11-1			107	110	22	8	25	24	32	9	18	2	6	15	378
G12-1			108	110	20	2	36	12	22	7	16	0	4	3	340
G12-2			110	102	24	6	29	32	22	12	12	4	6	8	367
G13-1			115	113	16	2	23	16	26	7	25	3	4	5	355
G14-1			145	95	8	0	11	13	30	3	14	4	9	22	354
G17 -1			138	102	15	0	1	25	43	4	14	4	9	25	380
G19			113	125	8	5	9	17	34	0	15	2	4	27	359
B3-1			117	133	13	3	1	15	23	7	10	10	0	26	358
B6			43	134	13	6	10	30	41	4	29	4	0	35	349
B8			39	174	8	11	13	29	33	6	54	1	0	29	397
B9		Bidestan Mb	44	198	15	9	22	20	16	1	31	3	0	31	390
B12			63	180	22	3	9	19	21	5	34	3	0	28	387
B14			68	177	8	6	17	20	15	5	50	4	1	20	391
B15			54	198	13	8	22	8	22	5	33	5	1	28	397
B16			63	183	7	12	8	8	14	2	48	1	4	21	371
Y6 -1			77	177	7	10	1	8	14	0	27	2	0	60	383
Y7-1			80	176	10	6	1	14	16	3	37	0	0	32	377
Y8 -1			72	198	10	1	0	16	16	5	38	1	3	15	375
Y9 -1	Yazd		90	163	5	2	0	24	13	0	40	2	7	16	362
Y12 -1			81	164	17	30	4	3	4	6	79	0	1	10	399
Y22 -1			53	181	25	4	3	8	2	25	33	1	2	40	380
Y24-1			64	174	17	15	2	4	0	53	32	3	2	30	396
M0			57	178	18	6	1	37	21	8	44	5	3	19	397
M1-1			47	165	15	15	3	23	24	4	46	3	4	9	358
M4-1			61	179	23	14	1	25	31	11	37	4	8	5	399
M5-1			57	221	10	6	0	18	24	13	32	10	8	0	399
M7-1			89	187	13	9	1	17	18	0	50	2	5	0	391
M11-1			44	207	8	5	4	12	32	8	16	15	8	4	363
M14-1		Qhrogchi	50	181	12	6	2	7	57	11	61	0	2	11	400
M16-1			63	199	8	8	7	9	16	0	45	1	7	17	380
M13-3			55	222	11	5	2	10	30	11	36	3	2	7	394
M18-1			66	201	6	2	11	11	20	3	52	2	6	19	399
M19-1			61	220	5	3	1	10	17	3	36	5	1	10	372
M24-1			29	236	13	2	3	15	28	11	28	7	3	24	399
M25-1			45	177	16	18	6	8	4	13	73	1	2	35	398
M26-1			82	190	14	13	3	9	6	19	25	0	2	21	384

Table 2: Modal analysis of 55 selected sandstone samples of the Nayband Formation, central Iran.

Sample No.	section and member		Q F RF (%)			Qm F Lt (%)			Qt F L (%)			Q F L (%)		
			Q	F	RF	Qm	F	Lt	Qt	F	L	Q	F	L
Q1-1	Dizlu	Qadir Mb	87	12	1	75	12	13	88	12	0	88	12	0
Q3-1			79	12	9	60	12	28	83	12	5	82	13	5
Q4-1			89	6	5	75	6	19	90	6	4	90	7	3
Q5-1			81	12	7	67	12	21	83	12	5	83	12	5
Q6-1			79	13	8	69	13	18	82	13	5	82	14	4
Q8-1			77	15	8	66	15	19	80	15	5	80	15	5
Q10-1			77	8	15	56	8	36	82	8	10	82	8	10
Q11-1			81	8	11	67	8	25	86	8	6	86	8	6
Q12-1			70	20	10	61	20	19	73	20	7	72	20	8
Q13-1			69	12	19	54	12	34	71	12	17	71	12	17
Q14-1			75	20	5	51	20	29	78	20	2	77	20	3
G2-1		Gelkan Mb	78	13	9	54	13	33	82	13	5	81	14	5
G3-1			80	14	6	62	14	24	84	14	2	84	14	2
G4-1			82	12	6	59	12	29	86	12	2	85	13	2
G5-1			82	12	6	57	12	31	86	11	3	86	12	2
G5-2			74	18	8	54	18	28	80	18	2	79	19	2
G5-3			81	13	6	65	13	22	84	13	3	84	13	3
G6-2			77	14	9	68	14	18	83	14	3	82	15	3
G7-1			74	19	7	66	19	15	78	19	3	77	20	3
G11-1			78	15	7	63	15	22	83	15	2	81	16	3
G12-1			83	10	7	66	10	24	88	10	2	87	11	2
G12-2			78	15	7	61	15	24	82	15	3	80	16	4
G13-1			79	12	9	67	12	21	86	12	2	85	13	2
G14-1			82	13	5	75	13	12	86	13	1	85	14	1
G17 -1			75	20	5	70	20	10	79	20	1	78	21	1
G19			80	16	4	73	16	11	84	16	0	84	16	0
B3-1		Bidestan Mb	83	12	5	77	12	11	86	12	2	86	12	2
B6			66	23	11	57	23	20	76	23	1	74	25	1
B8			63	21	16	55	21	24	77	21	2	74	24	2
B9			79	12	9	67	12	21	88	12	0	87	13	0
B12			77	13	10	64	13	23	86	13	1	85	14	1
B14			77	9	14	62	9	29	90	9	1	88	11	1
B15			79	8	13	68	8	24	91	8	1	89	9	2
B16			80	6	14	72	6	22	93	6	1	92	7	1
Y6 -1	Yazd		85	7	8	79	7	14	93	7	0	93	7	0
Y7-1			80	9	11	75	9	16	90	9	1	89	10	1
Y8 -1			79	9	12	76	9	15	90	9	1	88	10	2
Y9 -1			77	10	13	75	10	15	90	10	0	89	11	0
Y12 -1			78	2	20	65	2	33	97	2	1	96	2	2
Y22 -1			80	3	17	70	3	27	90	3	7	89	3	8
Y24-1			77	1	22	69	1	30	86	1	13	84	1	15
M0	Qhrogchi		67	20	13	60	20	20	78	20	2	75	23	2
M1-1			69	13	18	60	13	27	86	13	1	83	16	1
M4-1			72	15	13	63	15	22	82	15	3	81	16	3
M5-1			74	11	15	70	11	19	86	11	3	84	12	4
M7-1			78	9	13	72	9	19	91	9	0	90	10	0
M11-1			80	13	7	75	13	12	85	13	2	83	14	3
M14-1			65	17	18	60	17	23	80	17	3	77	20	3
M13-3			77	11	12	73	11	16	86	11	3	85	12	3
M16-1			80	7	13	74	7	19	93	7	0	92	8	0
M18-1			76	9	15	74	9	17	92	9	1	89	10	1
M19-1			81	8	11	79	8	13	91	8	1	91	8	1
M24-1			77	12	11	73	12	15	85	12	3	84	13	3
M25-1			72	4	24	63	4	33	92	5	3	91	4	5
M26-1			84	4	12	76	4	20	91	4	5	90	4	6

Table 3: Recalculated modal composition (in %) for the sandstones from the Nayband Formation, central Iran.

Asghar ETESAMPOUR, Asadollah MAHBOUBI, Reza MOUSSAVI-HARAMI, Nasser ARZANI & Mohammad Ali SALEHI

Sample No.	section and member		SiO_2	Al_2O_3	Fe_2O_3	MgO	CaO	Na_2O	K_2O	TiO_2	P_2O_5	MnO	LOI*	CIA	ICV	Sum
Q1-1	Dizlu	Qadir Mb	79.55	8.19	3.85	0.62	0.69	2.35	0.92	0.31	0.06	0.05	3.22	70.91	0.96	99.81
Q3-1			82.16	6.52	2.75	0.42	1.86	2.34	0.78	0.40	0.14	0.09	2.32	64.55	1.21	99.78
Q5-1			74.25	6.06	4.55	0.52	4.05	2.01	0.68	0.64	0.14	0.21	6.69	64.74	1.64	99.8
Q8-1			72.1	6.52	8.92	0.86	2.89	1.32	0.92	0.32	0.21	0.41	5.26	81.70	2.02	99.73
Q12-1			85.39	6.12	2.49	0.34	0.58	1.45	0.94	0.25	0.08	0.02	2.01	73.82	0.84	99.67
Q14-1			86.31	3.98	2.83	0.14	2.11	0.95	0.66	0.14	0.06	0.04	2.53	67.00	1.27	99.75
G2-1		Gelkan Mb	83.63	6.54	2.88	0.32	0.76	2.63	0.56	0.20	0.08	0.05	2.06	67.49	1.05	99.71
G4-1			89.25	4.85	1.22	0.04	1.65	2.38	0.39	0.10	0.01	0.02	1.23	52.89	1.12	99.86
G8-1			86.02	5.01	2.11	0.18	1.65	2.38	0.39	0.16	0.04	0.01	1.55	55.48	1.30	99.5
G12-1			85.66	5.36	1.66	0.25	0.46	2.11	0.62	0.16	0.04	0.01	3.52	65.77	0.87	99.85
G14-1			73.29	5.96	5.73	0.36	4.92	1.96	0.6	0.20	0.11	0.21	6.33	63.54	1.75	99.67
G15-1			80.39	6.68	3.54	0.46	2.62	2.31	0.56	0.20	0.07	0.09	2.78	59.86	1.33	99.7
G17-1			82.05	6.35	2.96	0.44	1.78	2.55	0.5	0.13	0.06	0.07	2.86	60.02	1.25	99.75
G19			83.01	6.98	2.02	0.53	0.92	2.76	0.83	0.29	0.12	0.03	2.24	67.83	0.94	99.73
B3-1		Bidestan Mb	78.36	7.65	2.72	0.39	2.92	2.71	0.85	0.19	0.03	0.04	4.01	56.17	1.15	99.87
B6			74.89	5.89	1.11	0.22	7.05	2.68	0.62	0.13	0.09	0.03	6.89	53.69	1.16	99.6
B9			71.49	4.12	0.98	0.15	10.77	1.84	0.5	0.05	0.04	0.03	9.67	52.15	1.19	99.64
B14			61.02	4.91	1.3	0.77	14.84	1.75	0.81	0.09	0.07	0.04	14.25	57.63	1.16	99.85
B16			59.11	4.11	1.07	1.48	15.83	1.72	0.51	0.06	0.11	0.05	15.68	59.05	1.48	99.73
Y4-1	Yazd		74.25	8.48	4.52	0.78	2.98	2.33	1.09	0.34	0.14	0.25	4.51	66.10	1.24	99.67
Y6-1			70.81	5.59	3.27	1.51	6.85	3.21	0.31	0.14	0.08	0.37	7.69	48.52	2.09	99.83
Y8-1			78.91	6.15	4.39	0.55	3.01	2.39	0.42	0.23	0.10	0.22	3.49	59.42	1.65	99.86
Y12-1			83.51	4.27	2.11	0.19	3.37	1.02	0.52	0.18	0.07	0.05	4.45	69.66	1.07	99.74
Y22-1			76.26	8.01	2.22	0.62	2.46	0.22	1.19	0.33	0.08	0.04	8.22	90.61	0.46	99.65
Y24-1			76.35	10.7	2.28	0.32	2.16	0.02	1.94	0.43	0.08	0.06	5.38	90.07	0.29	99.72
M1-1	Qhrogchi		71.25	9.71	5.66	0.95	0.63	2.05	1.38	0.41	0.06	0.06	7.6	73.73	1.01	99.76
M4-1			76.01	9.51	6.42	0.53	0.39	2.43	1.02	0.53	0.09	0.10	2.8	76.39	1.09	99.83
M7-1			85.39	6.01	2.85	0.48	0.28	2.34	0.46	0.27	0.04	0.01	1.54	69.16	1.04	99.67
M11-1			78.52	8.32	3.63	0.62	2.13	2.29	0.95	0.28	0.10	0.98	2.8	65.56	1.19	99.62
M14-1			80.56	9.12	2.87	0.59	0.52	2.69	0.94	0.33	0.07	0.03	1.71	72.55	0.77	99.43
M18-1			80.52	7.13	3.02	0.66	1.36	2.69	0.63	0.31	0.09	0.12	3.16	65.35	1.14	99.69
M21-1			73.25	7.23	4.32	1.12	4.19	2.28	0.96	0.25	0.08	0.11	5.96	60.50	1.43	99.75
M26-1			70.87	5.59	4.18	1.52	6.75	0.03	0.81	0.25	0.09	0.33	9.36	100	1.13	99.78
Average Dizlu section	Qadir Mb		79.96	6.23	5.01	0.6	2.03	1.73	0.81	0.35	0.11	0.13	3.67	70.46	1.32	99.63
	Gelkan Mb		82.89	5.96	5.96	0.32	1.84	2.38	0.55	0.18	0.07	0.06	2.82	61.61	1.19	99.83
	Bidestan Mb		68.97	5.33	1.43	0.6	10.28	2.14	0.65	0.11	0.07	0.04	10.1	55.74	1.22	99.72
Average Yazd section			76.68	7.19	3.13	0.66	3.47	1.53	0.91	0.28	0.09	0.15	5.62	70.73	1.13	99.71
Average Qhrogchi section			77.04	7.82	4.11	0.8	2.03	2.1	0.89	0.33	0.08	0.22	4.36	72.97	1.10	99.78

Table 4: Major elements (wt. %), CIA (Nesbitt and Young, 1982) and ICV (Cox et al., 1995) values of the studied sandstones from Nayband Formation, central Iran.

The results of geochemical analysis of the major elements in the studied sandstones plotted on Pettijohn et al. (1987) and Herron (1988) diagrams indicate litharenite, subarkose and sublitharenite petrofacies (Fig. 9A, B) and correlate with the petrographic data (Fig. 5).

5. Discussion

5.1 Source rock composition

5.1.1 Modal analysis

Plotting the modal data on the Tortosa et al. (1991) and Basu et al. (1975) diagrams indicates that the sandstones of the Nayband Formation originated from granitic, moderate to high-grade metamorphic rocks (Fig. 10A, B). The high ratio of monocrystalline to polycrystalline quartz can be caused by the destruction of primary polycrystalline quartz during high energy and long-term transportation (Folk, 1951). The presence of foliated metamorphic quartz in thin sections also emphasizes the metamorphic provenance. The high percentage of monocrystalline quartz with non-undulatory extinction suggests a plutonic provenance for the sandstones and the lack of fluid inclusions in the quartz gives evidence against a hydrothermal provenance (Basu et al., 1975).

sciendo

Sample No.	section and member			V	Zr	Sc	Sr	Ni	Ba	Cu	Co
Q1	Dizlu	Qadir Mb		55	69	5	29	114	8	11	39
Q8-1				110	70	8	32	131	7	14	42
Q12-1				38	56	<1	25	116	13	7	36
Q14-1				28	28	3	18	101	9	5	35
G2-1		Gelkan Mb		27	37	4	27	129	30	10	30
G8-1				30	61	3	17	72	18	5	52
G12-1				21	50	3	23	108	33	6	56
G15-1				70	38	3	20	112	27	7	29
G19				20	59	<1	13	86	9	5	28
G20-1				71	34	3	18	91	67	5	39
B2		Bidestan Mb		70	40	4	**21**	**154**	7	9	27
B3-1				103	55	<1	**43**	**94**	45	6	29
B9				11	29	<1	**13**	**176**	27	1	8
B14				25	34	<1	**10**	**91**	7	1	15
B16				14	29	<1	**9**	**72**	6	<1	11
B17-1				40	19	4	**12**	**73**	12	5	19
Y1	Yazd			59	69	4	153	29	184	10	13
Y4-1				50	41	6	165	29	178	19	13
Y8-1				56	33	7	219	27	93	11	11
Y12-1				53	28	5	110	25	101	32	10
Y24-1				95	49	8	60	23	293	6	10
M1-1	Qhrogchi			53	31	5	51	31	107	25	12
M7				30	65	<1	60	25	102	12	6
M11-1				53	42	6	79	35	145	28	12
M14-1				55	47	5	71	39	125	30	12
M18				62	90	2	108	33	102	13	11
M26-1				43	29	4	102	19	110	7	7
Average Dizlu section	Qadir Mb			57.75	55.75	5.33	63	26	9.25	9.25	38
	Gelkan Mb			39.83	46.5	3.2	71	19.66	30.67	6.3	39
	Bidestan Mb			43.83	34.33	4	**18**	**115**	17.33	3.8	18.17
Average Yazd section				62.6	44	6	141.4	26.6	169.8	15.6	17.2
Average Qhrogchi section				49.33	50.66	4.4	78.5	30.33	115.67	19.17	9

Table 5: Trace elements (ppm) concentration of the studied sandstones from Nayband Formation, central Iran.
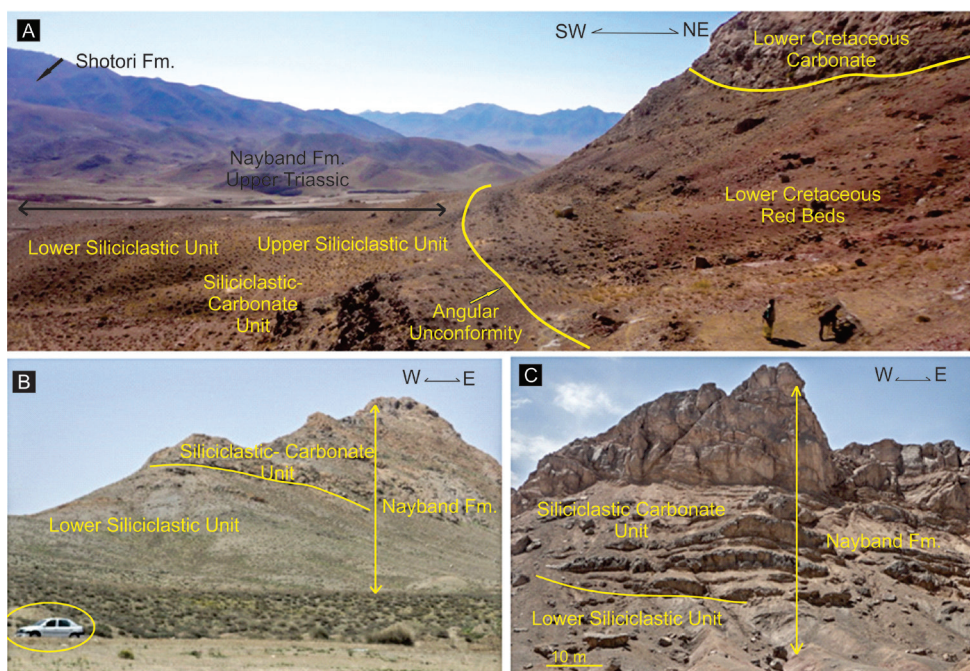

Figure 3: Field photos of the Nayband Formation in Central Iran. A: Overview of the Dizlu section from the three lithostratigraphic units of the Nayband Formation, inserted between the Middle Triassic Shotori carbonates and the overlying Lower Cretaceous red bed, B–C: The lower siliciclastic and middle siliciclastic-carbonate units of the Nayband Formation cropped out in desert, Qhrogchi and Yazd sections, respectively.
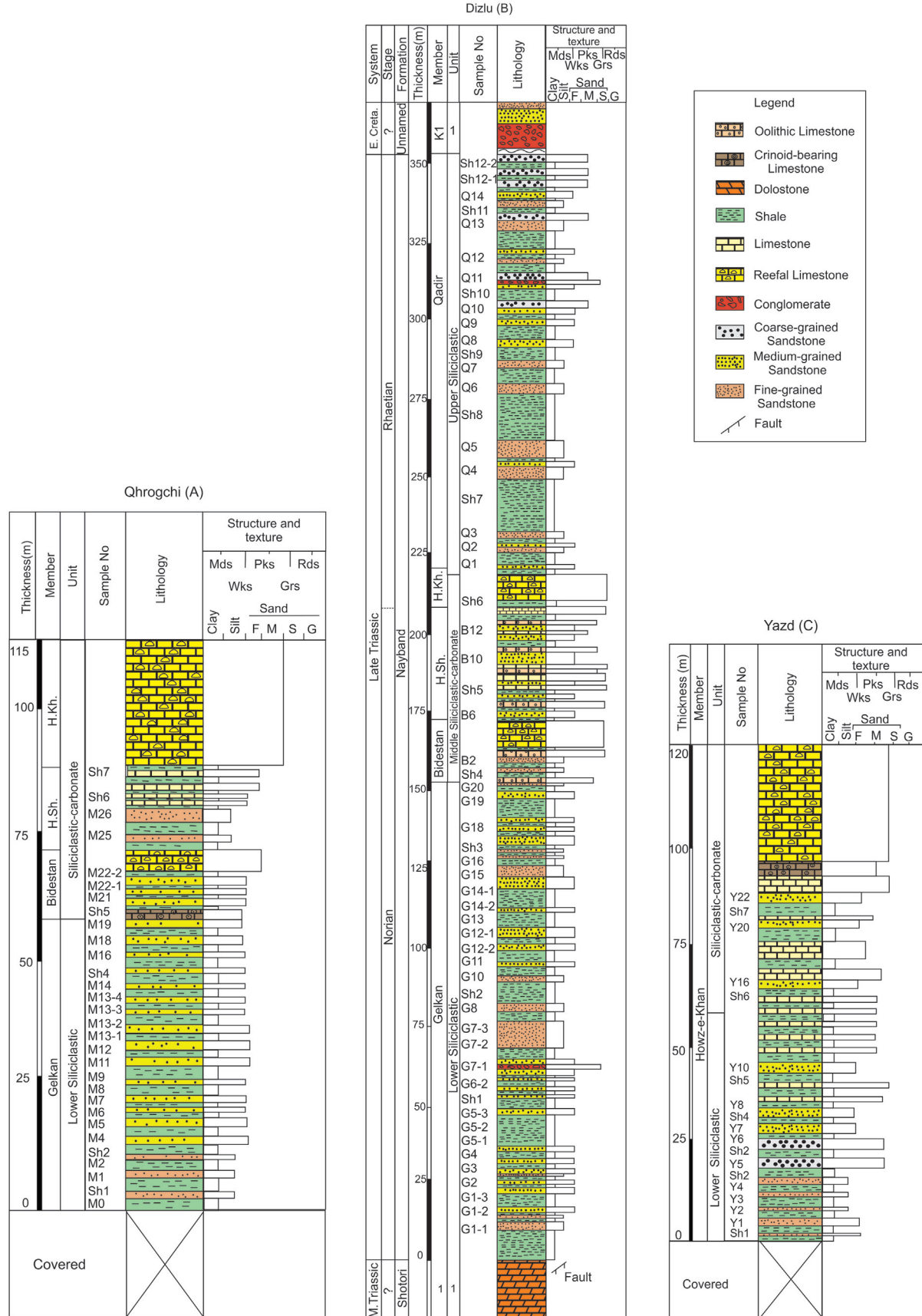
Figure 4: Lithostrigraphic logs of the Nayband Formation at Qhrogchi (A), Dizlu (B) and Yazd (C) sections, central Iran.

5.1.2 Geochemical analysis

Roser and Korsch (1988) have proposed the discriminant function diagram to distinguish the sediments concerning their primary source rock as mafic, intermediate and felsic igneous rocks or sediments containing quartz. In this function, major oxides including Al_2O_3, TiO_2, $Fe_2O_3^{total}$, CaO, MgO, K_2O and Na_2O are used as variables in the calculation. In this diagram, most of the samples of the Gelkan and Qadir members of the Nayband Formation at the Dizlu section are plotted in the quartz sedimentary provenance field while the Bidestan Member samples plot in the intermediate and felsic igneous

Figure 5: Microscopic photographs of the components of sandstones from the Nayband Formation. A: Monocrystalline quartz with undulos (Qm un) and straight extinctions (Qm nun), B: Altered microcline, C: Polycrystalline quartz (QP> 3), D: Altered potassium feldspar (K fel), E: Metamorphic quartz (Qmet), F: Metamorphic rock fragment (in XPL light).

fields. The Yazd section samples show positions in the intermediate igneous and sedimentary recycling fields and Qhrogchi section is dispersed in the same fields as the Dizlu and Yazd sections (Fig. 11A). Based on the discriminant function of the Roser and Korsch (1988) diagram the samples of the Qadir, Gelkan and Bidestan members at Dizlu section and the Qhrogchi section are fall within the felsic and intermediate igneous fields while, the Yazd section samples are only plotted in the intermediate igneous field (Fig. 11B). The obtained results from the two different discriminant function diagrams show felsic and intermediate igneous and sedimentary recycling provenance as the main sources in the studied sections. The major element composition on Taylor and McLennan (1985) diagram represents a granitic provenance (Fig. 11C). The geochemical proxies verify the results from the petrographic studies.
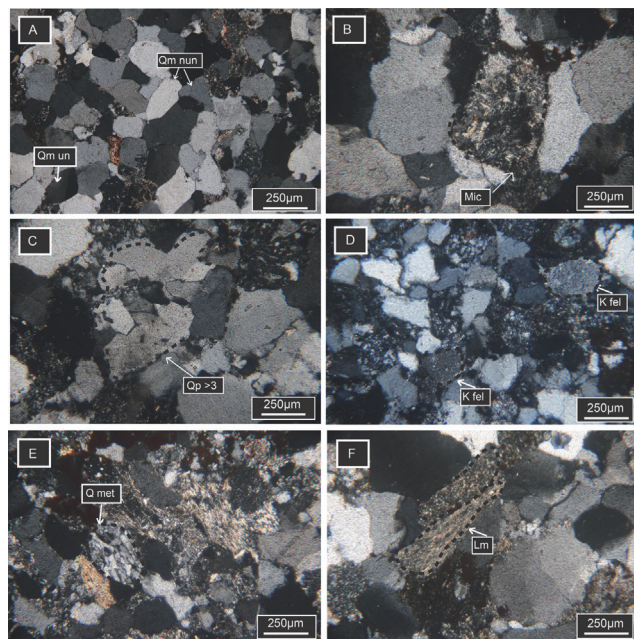
The studied sediments point to the exposure of supracrustal successions of the Cimmerian terranes due to the Eo-Cimmerian orogenic phase related to the central Iran and Turan continental collision during Late Triassic. These orogenic processes are considered as the main mechanisms for supplying sediment to the Nayband basin. The west-dipping Yazd Block may have been a likely source for the siliciclastic rocks which provided a mixed recycled provenance (e.g. Wilmsen et al., 2010).

The results of the trace elements analysis plotted on the McLennan et al. (1993) diagram indicate the post Archean field (Fig. 12A). The same elements plotted on the Floyd et al. (1989) diagram show an acidic source rock (Fig. 12B). The bivariate diagram of TiO_2 against Zr suggests that the source rocks of Nayband sediments were of felsic and intermediate provenance (Fig. 12C). Analysis of the source rock based on the modal and geochemistry as well as the petrofacies studies shows very close correspondence and overall felsic and intermediate igneous source rocks.
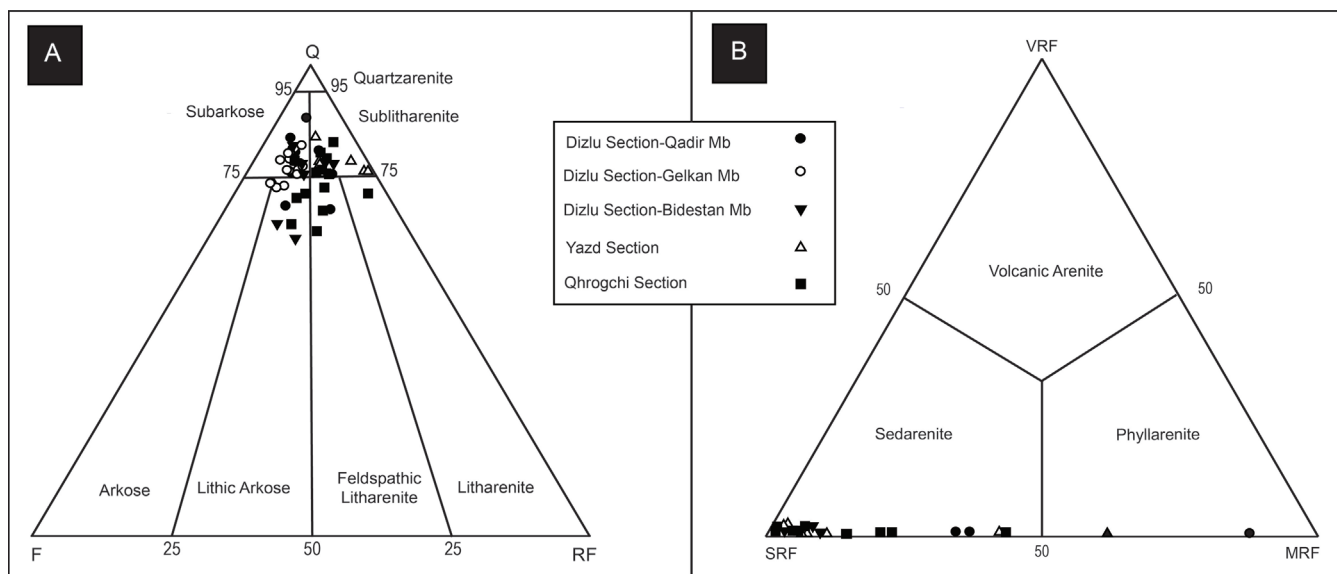

Figure 6: A and B: Sandstones classification (based on Folk, 1980) of samples from the Nayband Formation.
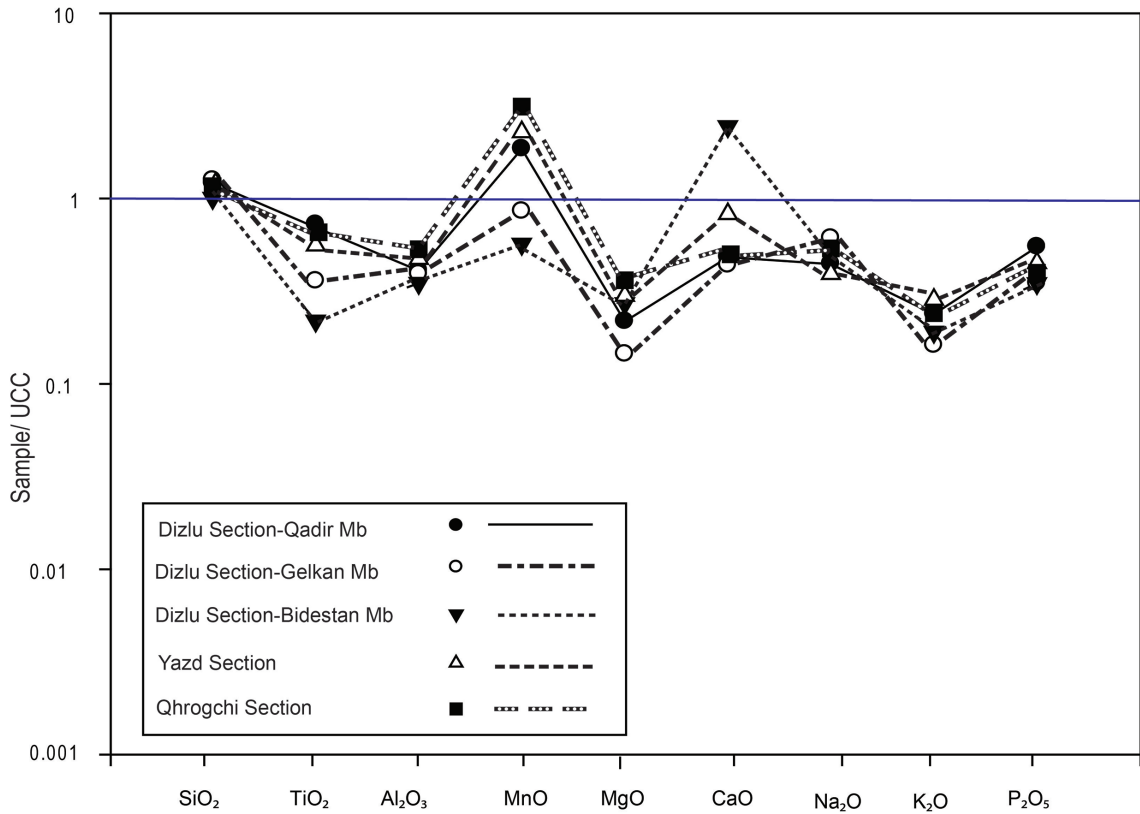
Figure 7: Normalization of major elements of the sandstones from the Nayband Formation relative to the UCC composition (Taylor and McLennan, 1985).
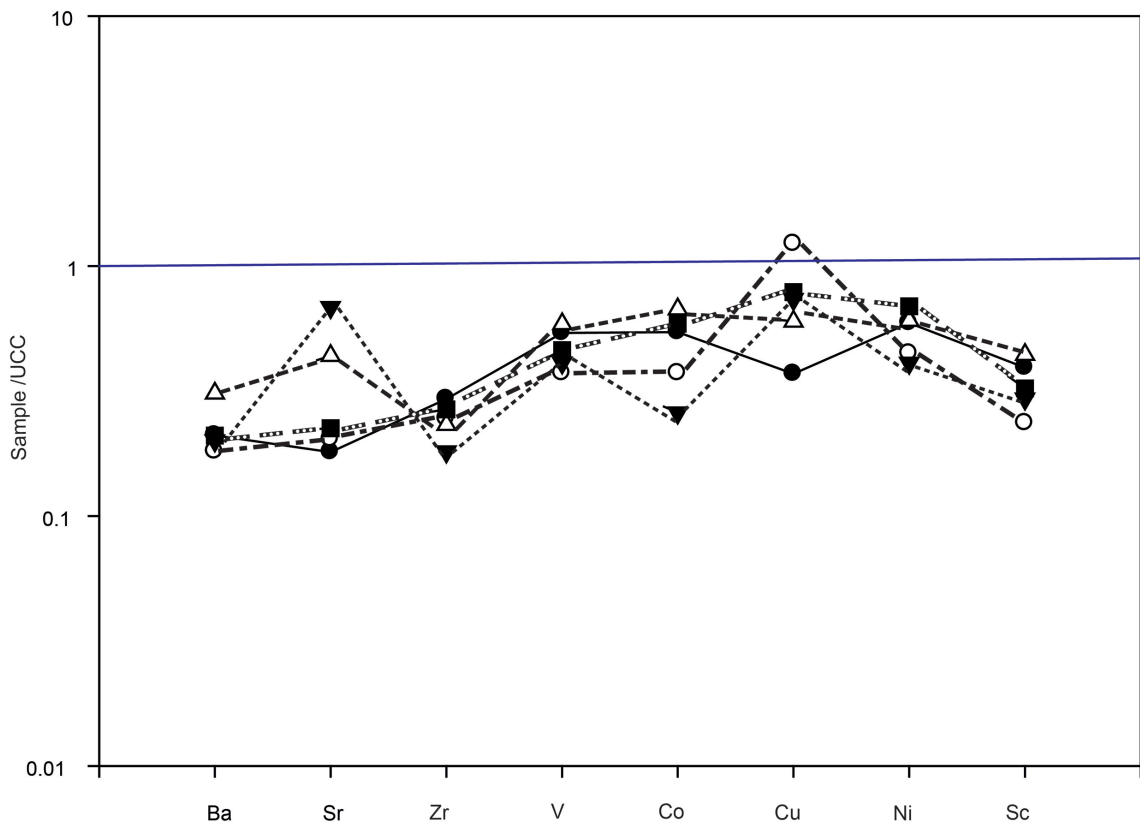

Figure 8: Normalization of trace elements of the sandstones from the Nayband Formation relative to the UCC composition (Taylor and McLennan, 1985) (refer to Fig. 7 for the symbol legend).
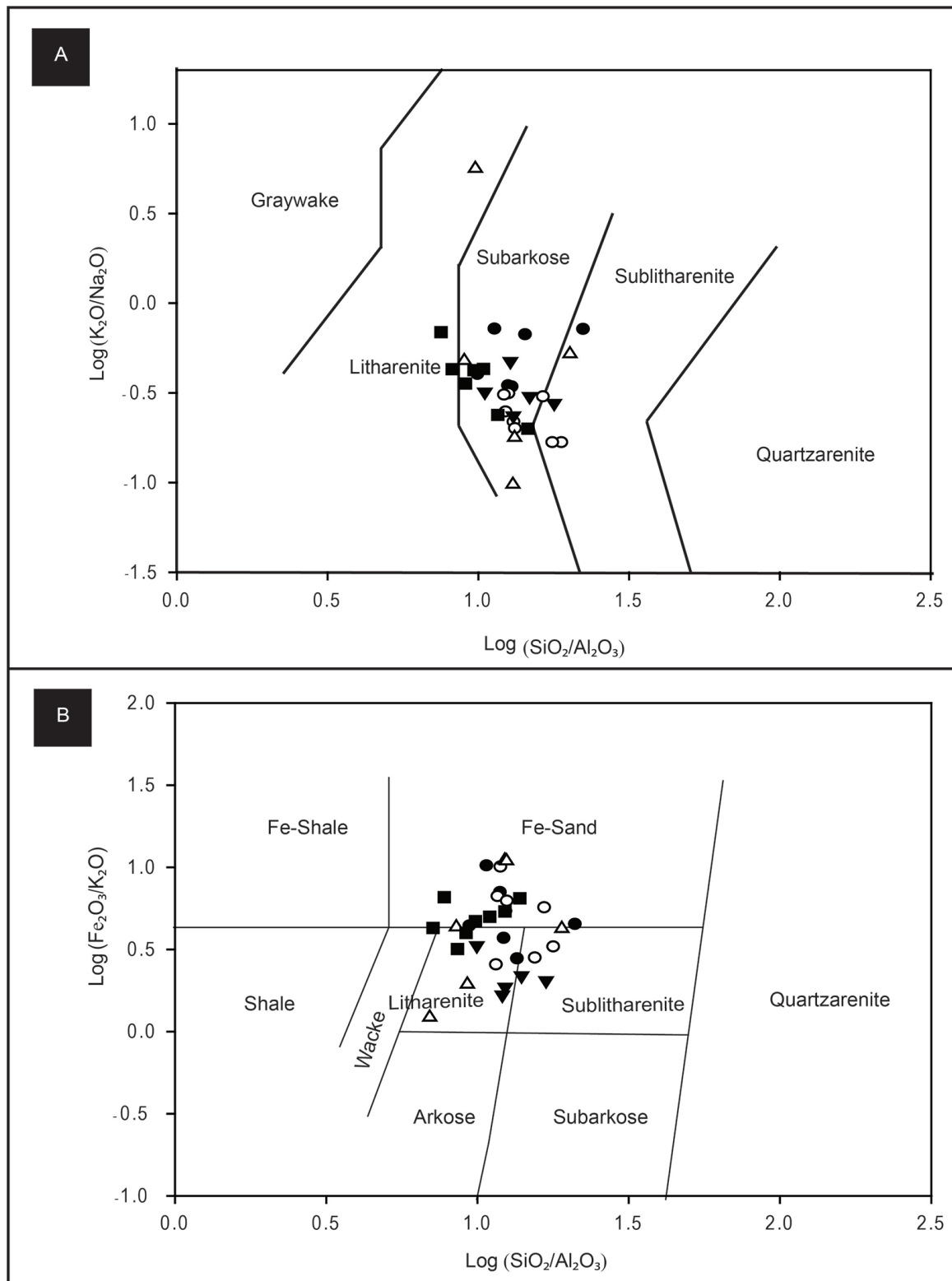
Figure 9: Geochemical classification of the sandstones of the Nayband Formation. A: Pettijohn et al. (1987), B: Herron (1988) (refer to Fig. 6 for the symbol legend).

5.2 Tectonic setting

5.2.1 Modal analysis

Tectonics and depositional setting have a direct effect on the sandstones composition, which is consequently used as a tool to reconstruct the general tectonic setting (Dickinson, 1985). The modal analysis of the composition of the studied sandstones at the Dizlu section in the Qm-FLt ternary diagram (Dickinson and Suczek, 1979) indicates that most samples of the Qadir Member plot in the recycled orogenic field; the Gelkan Member samples plot in the transitional-continental and craton interior fields;
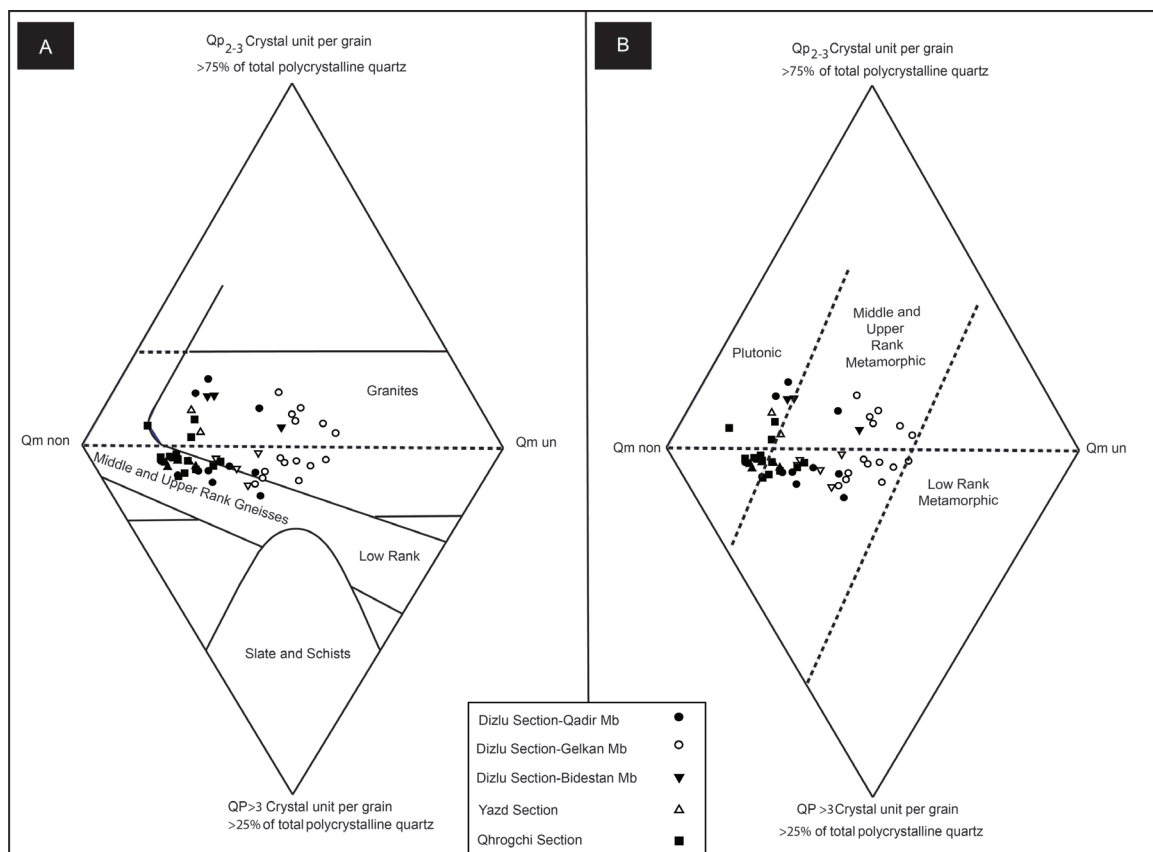
Figure 10: Quartz grains varieties of sandstones from the Nayband Formation. A: Tortosa et al. (1991), B: Basu et al. (1975) (refer to Fig. 6 for the symbol legend).

the Bidestan Member samples are distributed in the fields near the Qm pole; the Yazd section samples plot in the craton interior and recycled orogenic fields and the Qhrogchi section are just in the recycled orogenic field (Fig. 13A). Thus, the sandstone samples mainly plot in the recycled orogenic field and a few samples in the craton interior field in the QtFL ternary diagram (Dickinson, 1988) (Fig. 13B). The sandstones which plot in the craton field, near the triangle pole, are mature and have been transported long distances with frequent sedimentary recycling (Cox et al., 1995). Plotting the modal data of the sandstones on the Yerino and Maynard (1984) diagram (QFL) indicates passive continental margin setting for all samples (Fig. 13C).

5.2.2 Geochemical analysis

Geochemical studies of the major elements in the sandstones show that the composition of these rocks is closely related to the provenance and tectonic setting of the basin (North et al., 2005; Armstrong-Altrin et al., 2012). Plotting the data on the ternary diagram of Kroonenberg (1994) indicates that all the samples of the three sections plot in the passive continental margin (Fig. 14A). The values of TiO_2 plotted versus $MgO + Fe_2O_3$ on Bhatia (1983) diagram (Fig. 14B–D) represents that the data of Qadir and Gelkan members and also Yazd section indicate both active and passive continental margin fields; the Bidestan Member samples plot in the passive continental margin field and Qhrogchi

section samples are in the active continental margin field (Fig. 14B). Plotting the geochemical results on the Al_2O_3/SiO_2 versus $Fe_2O_3 + MgO$ graph indicates that all data of the three sections are located near the active continental margin field (Fig. 14C). The geochemical data of Qadir and Gelkan members, Yazd and Qhrogchi sections plotted on the $Al_2O_3 / (CaO + Na_2O)$ versus $Fe_2O_3 + MgO$ graph and are located in the boundary of the active and passive continental margin fields; and the Bidestan Member plots in the active continental margin field (Fig. 4D). Overlap of sample points into fields of passive and active continental margin suggests to use other criteria of discrimination. Crook (1974) reported that the sediments of passive continental margins are highly mature, originated in the plate interiors, intracratonic, and deposited on stable (passive) continental margins. In the present case, the Nayband Formation sediments mainly lack evidences for recycling and support deposition under an immature environment related to an area with active tectonism. The inferred active tectonic setting of the sediments is correlated with Late Triassic palaeogeography which will be discussed in the following.

5.3 Chemical weathering

The intensity of weathering is mainly controlled by the rock composition, climatic conditions and tectonic setting (Armstrong-Altrin et al., 2004; Garzanti and Resentini, 2016).
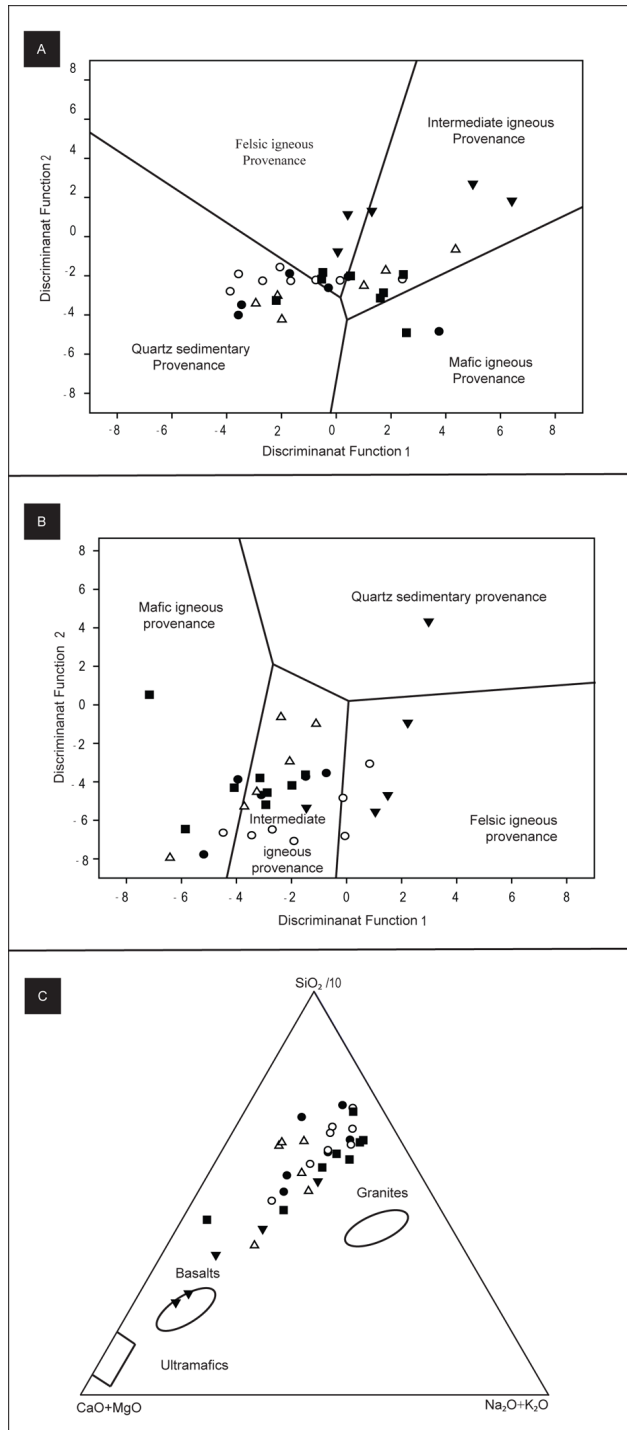
Figure 11: A: Discriminant function diagram (Roser and Korsch, 1988) based on major elements of of sandstone from the Nayband Formation. Discrimination function 1 = -1.773 TiO_2 + 0.607Al_2O_3 + 0.76 Fe_2O - 1.5 MgO + 0.616 CaO + 0.509 Na_2O - 1.224 K_2O - 9.09, Discrimination function 2 = 0.445 TiO_2 + 0.07 Al_2O_3 - 0.25 Fe_2O - 1.142 MgO + 0.438 CaO + 1.475 Na_2O + 1.426 K_2O - 6.861. B: Discriminant function diagram based on major element of Roser and Korsch (1988), Discrimination function1 = 30.638 TiO_2/Al_2O_3 − 12.541 Fe_2O_3 (t)/Al_2O_3 + 7.329 MgO/Al_2O_3 + 12.031 Na_2O/Al_2O_3 + 35.402 K_2O/Al_2O_3 − 6.382, Discrimination function 2 = 56.500 TiO_2/Al_2O_3 − 10.879 Fe_2O_3 (t)/Al_2O_3 + 30.875 MgO/Al_2O_3 − 5.404 Na_2O/Al_2O_3 + 11.112 K_2O/Al_2O_3 − 3.89. C: The diagram of Taylor and Mc-Lennan (1985) for determining the source rock (refer to Fig. 6 for the symbol legend).
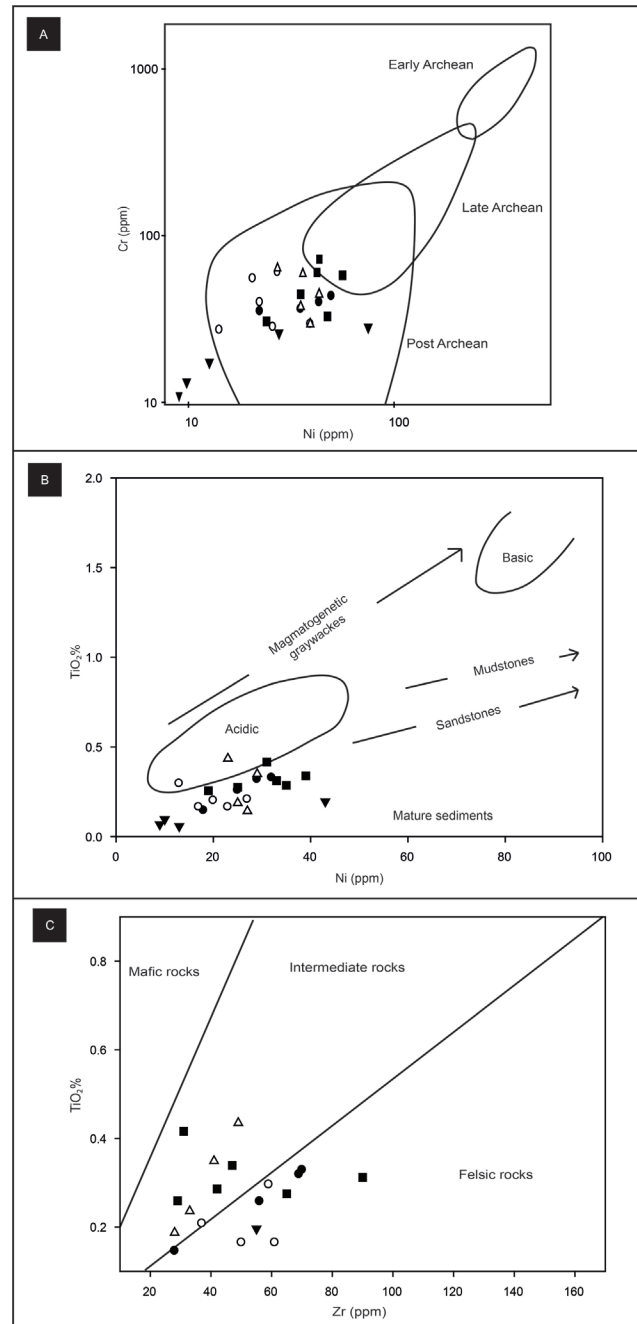

Figure 12: Plots of major and trace elements analysis data of sandstones from the Nayband Formation. A: Cr versus Ni (McLennan et al., 1993), B: TiO_2 versus Ni (Floyd et al., 1989), C: TiO_2 versus Zr bivariate diagram (Hayashi et al., 1997); (refer to Fig. 6 for the symbol legend).

5.3.1 Modal analysis

Modal data of the sandstones on the Weltje et al. (1998) diagram represent metamorphic and sedimentary source rock with the data having a tendency toward the plutonic field (Fig. 15A). In addition to determining the source rock of siliciclastic sediments, the above diagram defines the index of weathering which is previously presented by Grantham and Velbel (1988). The studied sandstones are located in fields number 1 and 2 in this diagram
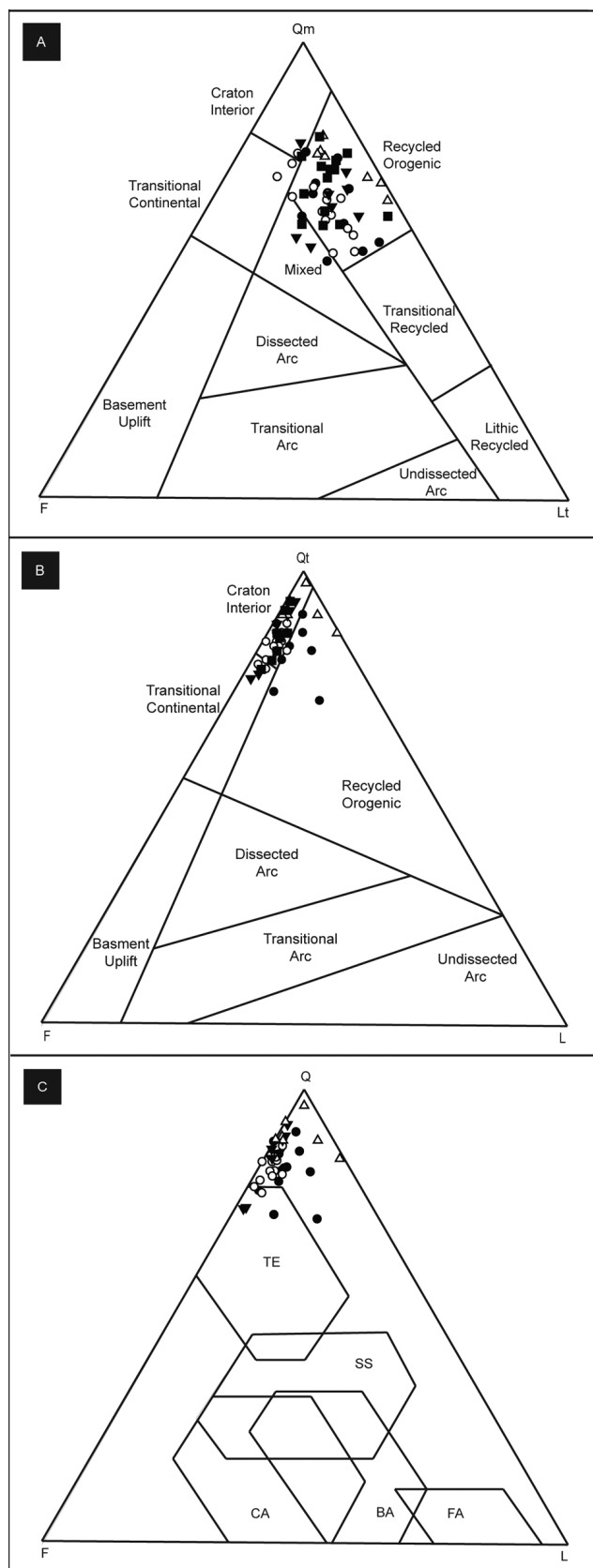
Figure 13: A: QtFL (Dickinson and Suczek, 1979), B: QmFLt (Dickinson, 1988) and C: QFL (Yerino and Maynard, 1984) plots showing tectonic provenance of sandstones from the Nayband Formation. TE: Passive Continental Margin, SS: Strike Slip, CA: Continental Arc, BA: Back Arc, FA: Fore Arc (refer to Fig. 6 for the symbol legend).

and show semi-humid and tropical conditions. Plotting the modal data on Suttner and Dutta (1986) indicates semi-humid climate for the Bidestan Member samples of Dizlu section and samples of the Yazd and Qhrogchi sections. A slight tendency from semi-humid toward the humid field is seen in the Qadir and Gelkan members of the Dizlu section (Fig. 15B). The results of the plotted data on the Suttner et al. (1981) diagram indicates plutonic and metamorphic source rocks and also points to a humid climate for the samples of all three sections (Fig. 15C).

5.3.2 Geochemical analysis

The chemical maturity of the sandstones is a function of the climate. The Suttner and Dutta (1986) diagram has been used to study the palaeoclimatic conditions in the sediments of the source area which indicates humid climate for the sandstones of all three sections. It should be noted that sandstones of the Qadir and Gelkan members of the Dizlu section have a stronger tendency to more humid climate condition (Fig. 16).

The obtained results correlate well with the petrographic data which show high amounts of quartz as a result of humid climate conditions. This climatic situation is also supported by palynoflora studies by Sajjadi et al. (2015) in southeastern Tabas implying a moist warm climate, and by the provenance analysis of the Upper Triassic sandstones from north of Isfahan (Salehi et al. 2018a). However, based on palynological study by Cirilli et al. (2005) on the Nayband Formation at the type locality, a change from humid to drier and warmer (tropical to subtropical) conditions is recorded. A warm, semiarid to arid palaeoclimate was also reported towards the east, in the Tethyan Salt Range of Pakistan, formerly situated in the southwestern Tethyan realm during Rhaetian (Iqbal el al., 2019).

5.3.2.1 Chemical Index of Alteration (CIA)

The CIA is a suitable method to evaluate the degree of chemical weathering and palaeoclimatic fluctuations (Nesbitt and Young, 1982; Bahlburg and Dobrzinski, 2011; Iqbal et al., 2019) which can be calculated by the following equation: CIA= $[Al_2O_3/(Al_2O_3+CaO^*+Na_2O+K_2O)]$ ×100. Where CaO* represents the Ca in silicate fractions and the samples with the high content of CaO is related to the diagenetic cement and must be corrected according to the following equation (e.g. Fedo et al., 1995): CaO* = CaO- (10.3 × P_2O_5). If the obtained CaO was less than Na_2O, no correction is needed; if it was more than Na_2O, we consider CaO equal to Na_2O (McLennan et al., 1993). The average value of CIA is 70.5 for the sandstones of Qadir Member, 61.6 for the Gelkan Member, 55.7 for the Bidestan Member at Dizlu section; 70.7 for Yazd and 72.9 for the Qhrogchi section (Table 4). We can attribute the low to moderate weathering to the relatively low amounts of fully altered feldspars which
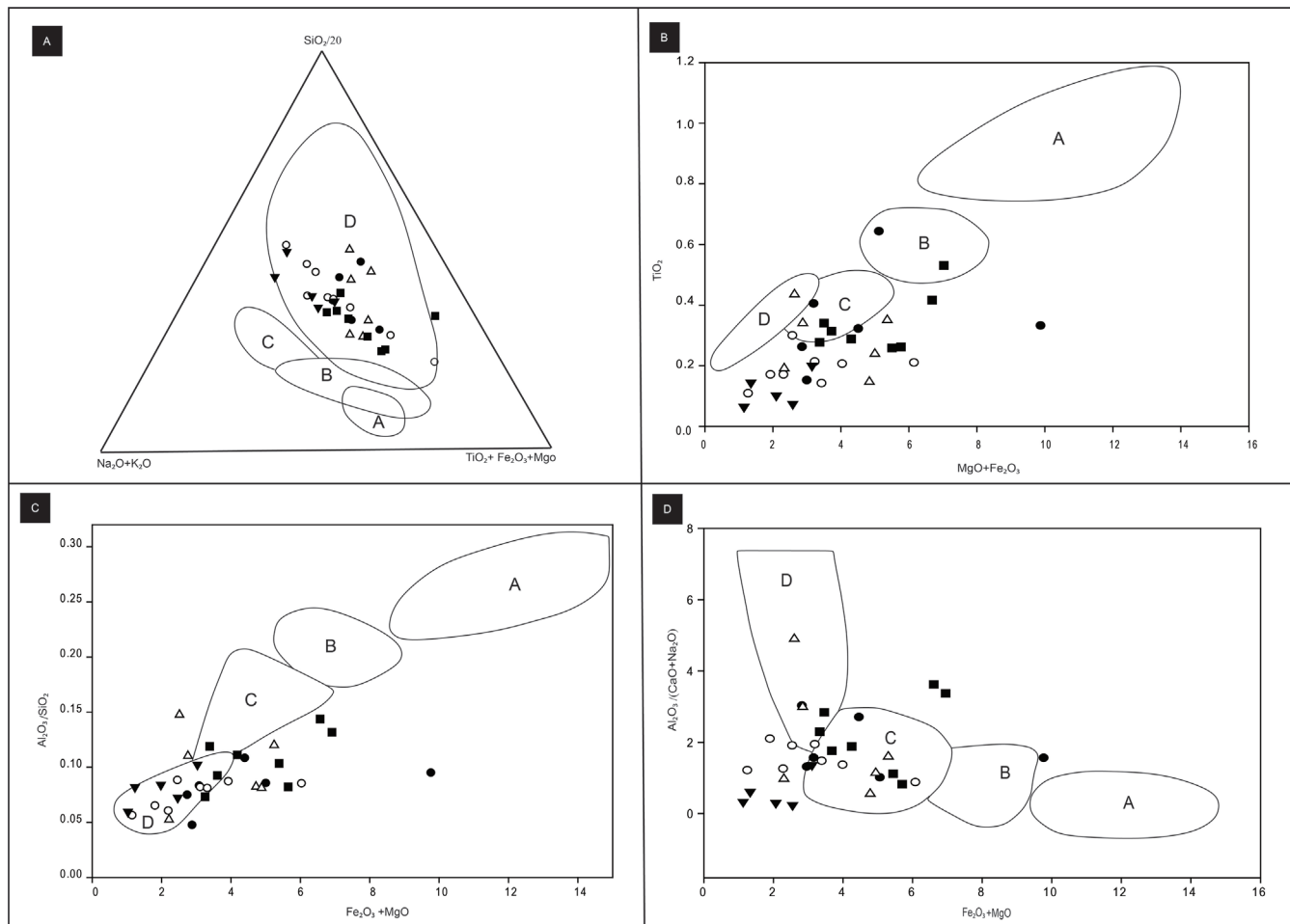
Figure 14: Tectonic setting of sandstone samples based on the major element from the Nayband Formation. A: Kroonenberg (1994), B–D: Bhatia (1983), A: Oceanic island arc, B: Continental island Arc, C: Active continental margin, D: Passive continental margin (refer to Fig. 6 for the symbol legend).

is closely correlated with the inferred tectonic setting. The slightly depleted mobile major and trace elements of the sandstone samples from the Nayband Formation relative to UCC also point to low to moderate weathering (Figs. 7, 8).

5.3.2.2 Index of Compositional Variability (ICV)

This index is used to determine the compositional maturity of sediments (Cox et al., 1995) and measures the abundance of aluminum compared to the other main cations in a rock or mineral by following equation: $ICV=[(CaO+K_2O+Na_2O+Fe_2O_3(t)+MgO+MnO+TiO_2)/Al_2O_3]$. The samples with higher alteration products such as clay minerals have less ICV values (less than 1) and are formed in the areas with very low topography and intense chemical weathering (Cullers and Podkovyrov, 2000). The average amount of the index is 1.3 in the Qadir Member, 1.9 in the Gelkan Member, 1.2 in the Bidestan Member at the Dizlu section; 1.1 at Yazd and 1.1 in the Qhrogchi section. The average of these results is higher than 1 and indicates compositionally immature and first-cycle deposits. Plotting the CIA data versus ICV (Lee, 2002; Potter et al., 2005) indicates moderate chemical weathering in the source area and minor sedimentary recycling for the studied samples (Fig. 17A). Most of the samples in the three sections are

near to the granitic source which shows low sedimentary recycling. We use the A–CN–K triangle diagram to determine the weathering trend of elements with molar proportions (Nesbitt and Young, 1982). Plotting data parallel to A–CN line indicates early stages of weathering (Fig. 17B). Based on the obtained results, the sandstone samples of Bidestan Member at the Dizlu section have experienced less weathering intensities compare to other samples.

5.4 Palaeogeographic implications

During the late Mid-Triassic (Ladinian) the northward drift of the Iran Plate resulted in narrowing of the Palaeotethys and Neotethys spreading (e.g. Wilmsen et al., 2009a) (Fig. 18A). The Shotori/Elikah carbonate platform was formed on a passive margin that covered a large area including the central Iran and the Alborz Basin (Aghanabati, 2004). Following the initial collision in the early Carnian, the northern margin of the Iran Plate was transformed into a peripheral foreland basin in northern Iran, forming a widespread hiatus and erosional unconformity in major areas of central Iran (Wilmsen et al., 2009a) (Fig. 18B). The deposition of the Nayband Formation (mid-Norian–Rhaetian) in CEIM occurred along an active continental margin following the Neotethys subduction and at the same time the lower Shemshak Group
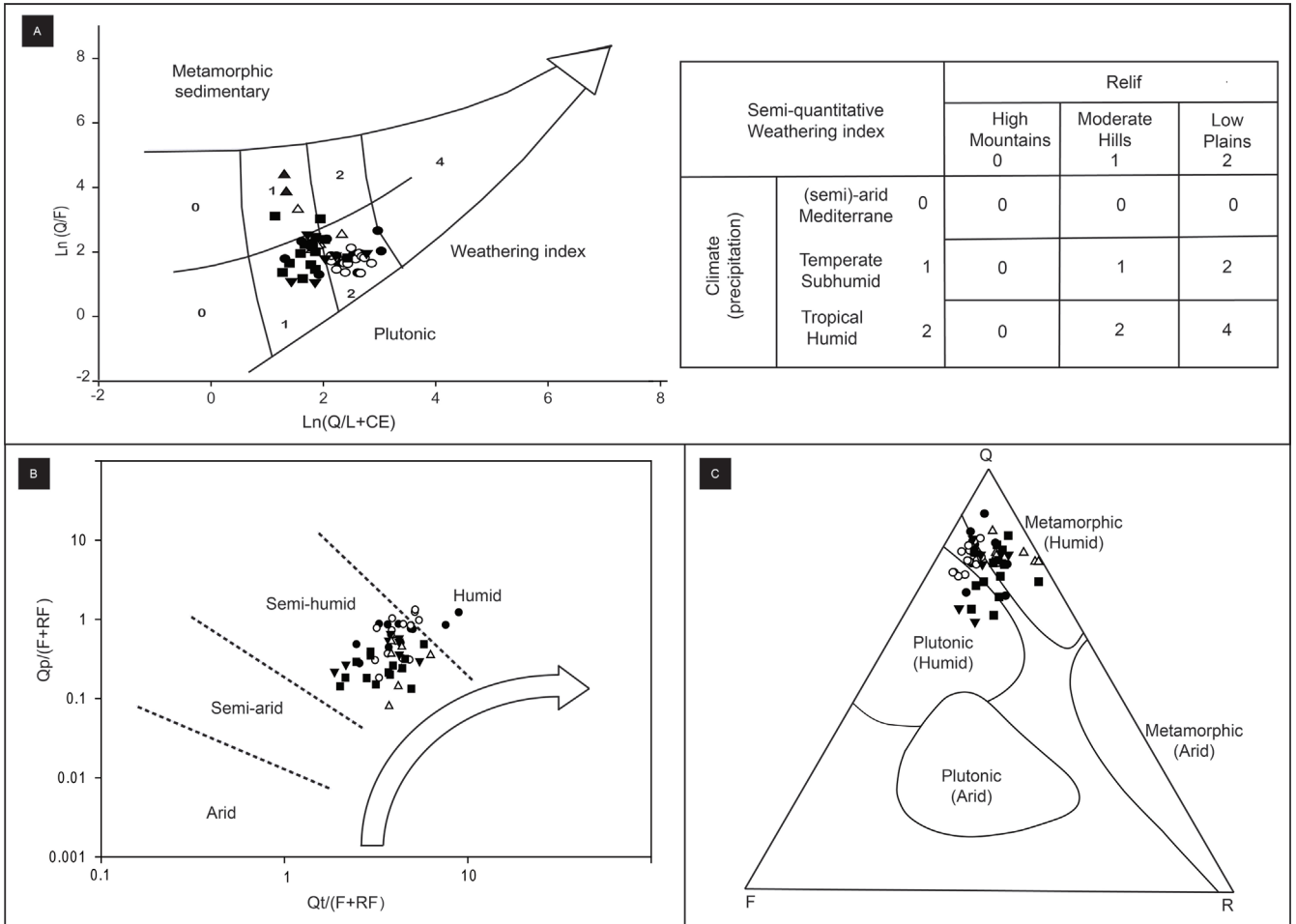
Figure 15: The modal data of sandstone samples from the Nayband Formation in the weathering diagrams. A: Weltje et al. (1998) (CE: Carbonate Elements), B: Suttner and Dutta (1986), C: Suttner et al. (1981) (refer to Fig. 6 for the symbol legend).
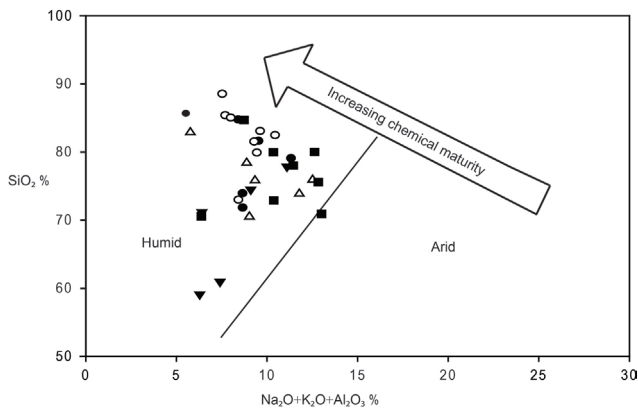

Figure 16: Plots the geochemical results of sandstone samples from the Nayband Formation on the palaeoclimate diagram (Suttner and Dutta, 1986) (refer to Fig. 6 for the symbol legend).

was deposited on a peripheral foreland basin in northern Iran (Alborz Basin) (Fig. 18C) (Wilmsen et al., 2009a, b). Thickness variations and facies development of the Nayband Formation in the study area are explained by a tilted fault block model in an extensional tectonic regime for the back-arc basin (Wilmsen et al., 2009b, 2010; Cifelli et al., 2013) (Fig. 18C). Such a Cimmerian-related

back-arc extensional tectonic pulses was documented in CEIM during the Late Triassic to Late Jurassic (Fürsich et al., 2005; Wilmsen et al., 2009a; Salehi et al., 2018b). A similar geodynamic setting has been offered for the CEIM and its southwestern margin (studied sections) in the geodynamic model of Cimmerian orogeny and the Triassic–Jurassic evolution of the Iran Plate (Wilmsen et al., 2009a). The extensional pulse in the Late Triassic resulted in block faulting with regional differences in subsidence and synsedimentary block movements that produced basins separated by shoulder uplifts (Fürsich et al., 2005). The Yazd Block remained topographically high during the Late Triassic to Early-to-Late Jurassic (Wilmsen et al., 2009b). An extensional tectonic setting has also been reported in the southwestern Tethyan realm, currently form northwestern Pakistan, by seismic data pointing to the presence of many subsurface basement normal faults. These faults formed due to rifting within Pangaea during the Triassic–Jurassic boundary interval and resulted in the breakup of the Indian Plate from Africa and Arabia (Iqbal et al., 2015a, b; 2019). Accordingly, the geochemical and modal analysis results of this study point to an active continental margin tectonic setting
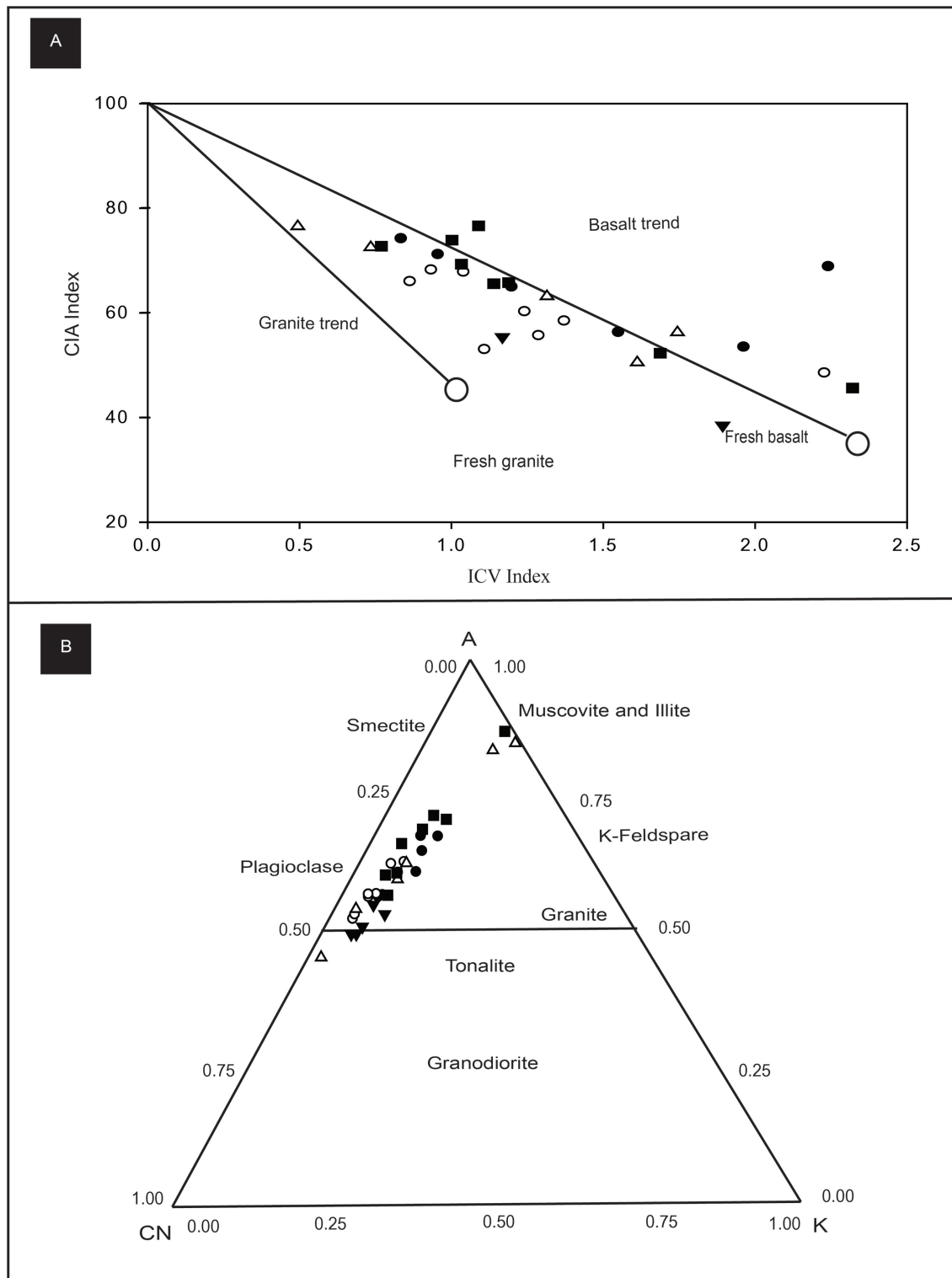
Figure 17: A: CIA versus ICV diagram indicates moderate chemical weathering and low sedimentary recycling for sandstone samples from the Nayband Formation (Lee, 2002; Potter et al., 2005), B: Diagram of A–CN–K (Al_2O_3 – CaO + Na_2O – K_2O) indicates low to moderate weathering stages (Nesbitt and Young, 1982) (refer to Fig. 6 for the symbol legend).

for the siliciclastic sediments of the Nayband Formation during the Late Triassic.

6. Conclusions

The petrography and geochemical studies of the siliciclastic deposits of the Upper Triassic Nayband Formation in Central Iran, led to the determination of the source rocks, tectonic setting, palaeoweathering and palaeoclimatic conditions:

The composition of sandstones in this formation shows a variety of quartz-rich petrofacies including sublitharenite (often subchertarenite), subarkose, lithic arkose,
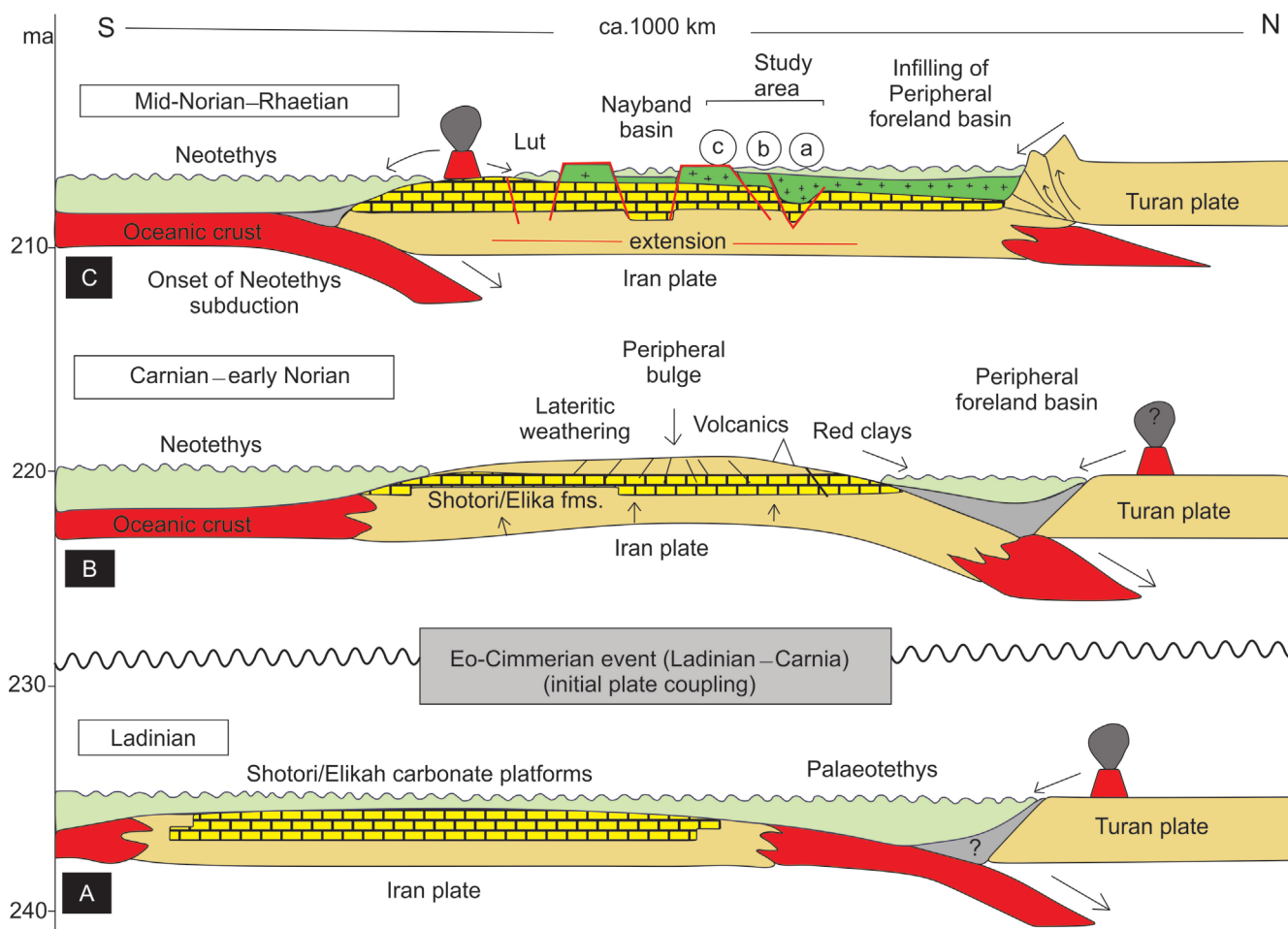
Figure 18: Geodynamic model for the Eo-Cimmerian orogeny in Iran (modified from Wilmsen et al., 2009a). A: The northward drift of the Iran Plate, B: The initial collision of the Iran Plate with Turan Plate, C: The deposition of the Nayband Formation (mid-Norian–Rhaetian) in southwestern margin of CEIM in an active continental margin following the Neotethys subduction. The approximate positions of the studied sections are indicated. a: Qhrogchi, b: Dizlu, c: Yazd sections.

feldspathic litharenite and litharenite and their components consist of more than 77% of various types of quartz, and minor feldspar and rock fragment.

Geochemical studies of major oxides, trace elements and modal analysis of the sandstones indicate mixed sedimentary, intermediate to felsic igneous rocks and moderate to high-grade metamorphic rocks in the source area. The results of major and trace elements geochemical studies give evidence for an active continental margin tectonic setting.

The study of the palaeoclimatic conditions based on the modal and geochemical analysis of the sandstone indicates humid to semi-humid climate in the source area with metamorphic and plutonic source rocks. The weathering of the source rocks based on geochemical analysis represents low to moderate weathering conditions.

The exposure of supracrustal successions of the Cimmerian terranes due to extensionally tilted fault blocks during the Late Triassic is considered as the main processes for supplying siliciclastic sediments to the Nayband basin.

Acknowledgments

References

Adhikari, B.R. and Wagreich, M., 2011. Provenance evolution of collapse graben fill in the Himalaya - The Miocene to Quaternary Thakkhola-Mustang graben (Nepal). Sedimentary Geology, 233, 1–14. https://doi.org/10.1016/j.sedgeo.2010.09.021

Aghanabati, S.A., 2004. Geology of Iran. Geological Survey of Iran, Tehran. 587 pp. (in Persian)

Armstrong-Altrin, J. S., Lee, Y., Verma, S. and Ramasamy, S., 2004. Geochemistry of sandstones from the Upper Miocene Kudanul Formation, southern India. Implications for provenance, weathering and tectonic setting.

Journal of Sedimentary Research, 74, 167–179. https://doi.org/10.1306/082803740285

Armstrong-Altrin, J.S., Lee, Y.I., Kasper-Zubillaga, J.J., Carranza-Edwards, A., Garcia, D., Eby, G.N., Balaram, V. and Cruz-Ortiz, N.L., 2012. Geochemistry of beach sands along the western Gulf of Mexico, Mexico: Implication for provenance. Chemie der Erde - Geochemistry, 72/4, 345–362. https://doi.org/10.1016/j.chemer.2012.07.003

Arribas, J., Critelli, S. and Johnsson, M.J., 2007. Sedimentary provenance and petrogensis: perspectives from petrography and geochemistry. Geological Society of American, Special Paper, 420, 396 pp. https://doi.org/10.1130/SPE420

Arvin, M., Pan, Y., Dargahi, S., Malekizadeh, A. and Babaei, A., 2007. Petrochemistry of the Siah-Kuh granitoid stock southwest of Kerman, Iran: Implications for initiation of Neotethys subduction. Journal of Asian Earth Sciences, 30/3–4, 474–489. https://doi.org/10.1016/j.jseaes.2007.01.001

Bahlburg, H. and Dobrzinski, N., 2011. A review of the Chemical Index of Alteration (CIA) and its application to the study of Neoproterozoic glacial deposits and climate transitions. Geological Society, London, Memoirs, 36/1, 81–92. https://doi.org/10.1144/M36.6

Basu, A., Young, S., Suttner, L., James, W. and Mack, G.H., 1975. Re-evaluation of the use of undulatory extinction and crystallinity in detrital quartz for provenance interpretation. Journal of Sedimentary Petrology, 45, 873–882. https://doi.org/10.1306/212F6E6F-2B24-11D7-8648000102C1865D

Bhatia, M.R., 1983. Plate tectonics and geochemical composition of sandstones. The Journal of Geology, 91, 611–627. https://doi.org/10.1086/628815

Bayet-Goll, A., de Carvalho, C.N., Daraei, M., Monaco, P. and Sharafi, M., 2018. Sequence stratigraphic and sedimentologic significance of the trace fossil Rhizocorallium in the Upper Triassic Nayband Formation, Tabas Block, Central Iran. Palaeogeography, Palaeoclimatology, Palaeoecology, 491, 196–217. https://doi.org/10.1016/j.palaeo.2017.12.013

Cifelli, F., Mattei, M., Rashid, H. and Ghalamghash, J., 2013. Right-lateral transpressional tectonics along the boundary between Lut and Tabas blocks (Central Iran). Geophysical Journal International, 193, 1153–1165. https://doi.org/10.1093/gji/ggt070

Cirilli, S., Buratti, N., Senowbari-Daryan, B. and Fürsich, F.T., 2005. Stratigraphy and palynology of the Upper Triassic Nayband Formation of East-Central Iran. Rivista Italiana di Paleontologia e Stratigrafia, 111/2, 259–270. https://doi.org/10.13130/2039-4942/6312

Cox, R., Lowe, D.R. and Cullers, R.L., 1995. The influence of sediment recycling and basement composition on evolution of mudrock chemistry in the southwestern United States. Geochimica et Cosmochimica Acta, 59, 2919–2940. https://doi.org/10.1016/0016-7037(95)00185-9

Crook, K.A.W., 1974. Lithogenesis and geotectonics: the significance of compositional cariations in flysch arenites (graywackes). In: R.H.Jr. Dott and R.H. Shaver (eds.),

Modern and Ancient Geosynclinals Sedimentation. Society for Sedimentary Geology Special Publication, 19, pp. 304–310.

Cullers, R.L. and Podkovyrov V.N., 2000. The source and origin of terrigenous sedimentary rocks in the Mesoproterozoic Ui group, southeastern Russia. Precambrian Research, 117, 157–183. https://doi.org/10.1016/S0301-9268(02)00079-7

Dickinson, W.R. and Suczek, D.R., 1979. Plate tectonics and sandstone compositions. American Association of Petroleum Geologists Bulletin, 63, 2164–2182.

Dickinson, W.R., 1985. Interpreting provenance relations from detrital modes of sandstones. In: G.G. Zuffa (ed.), Provenance of Arenites. Nato Science Series C: Mathematical and Physical Sciences, 48. Springer, Amsterdam, pp. 333–361. https://doi.org/10.1007/978-94-017-2809-6_15

Dickinson, W.R., 1988. Provenance and sediment dispersal in relation to paleotectonics and paleogeography of sedimentary basins. In: K.L. Kleinspehn and C. Paola, (eds.), New perspectives in basin analysis. Springer, New York, pp. 3–25. https://doi.org/10.1007/978-1-4612-3788-4_1

von-Eynatten, H., Barceló-Vidal, C. and Pawlowsky-Glahn, V., 2003. Composition and discrimination of sandstones: a statistical evaluation of different analytical methods. Journal of Sedimentary Reseach, 73, 47–57. http://dx.doi.org/10.1306/070102730047

Fathy, D., Wagreich, M., Zaki, R., Mohamed, R.S.A. and Gier, S., 2018. Geochemical fingerprinting of Maastrichtian oil shales from the Central Eastern Desert, Egypt: Implications for provenance, tectonic setting, and source area weathering. Geological Journal, 53/6, 2597–2612. https://doi.org/10.1002/gj.3094

Fedo, C.M., Wayne Nesbitt, H. and Young, G.M., 1995. Unraveling the effects of potassium metasomatism in sedimentary rocks and paleosols, with implications for paleoweathering conditions and provenance. Geology, 23/10, 921–924.

Floyd, P.A., Franke, W., Shail, R. and Dorr, W., 1989. Geochemistry and tectonic setting of Lewisian clastic metasediments from the Early Proterozoic Loch Maree Group of Gairloch, NW Scotland. Precambrian Research, 45, 203–214. https://doi.org/10.1016/0301-9268(89)90040-5

Folk, R.L., 1951. Stages of textural maturity in sedimentary rocks. Journal of Sedimentary Petrology, 21, 127–130.

Folk, R.L., 1980. Petrology of Sedimentary Rocks (2nd edition). Hemphill, Texas, 170 pp.

Fürsich, F.T., Brunet, M.-F., Auxiètre, J.-L. and Munsch, H., 2017. Lower–Middle Jurassic facies patterns in the NW Afghan–Tajik Basin of southern Uzbekistan and their geodynamic context. In: M.-F. Brunet, T. McCann and E.R. Sobel (eds.), Geological Evolution of Central Asian Basins and the Western Tien Shan Range. Geological Society, London, Special Publications. Geological Society, London, 427, pp. 357–409. http://doi.org/10.1144/SP427.9

Fürsich, F.T., Hautmann, M., Senowbari- Daryan, B. and Seyed-Emami, K., 2005. The Upper Triassic Nayband and

Darkuh Formations of east-central Iran. Stratigraphy, facies patterns and biota of extensional basins on an accreted terrane. Beringeria, 35, 53–133.

Fürsich, F.T., Wilmsen, M., Seyed-Emami, K. and Majid-ifard, M.R., 2009. The Mid-Cimmerian tectonic event (Bajocian) in the Alborz Mountains, Northern Iran: evidence of the break-up unconformity of the South Caspian Basin. In: M.-F. Brunet, J.W. Granath and M. Wilmsen (eds.), South Caspian to Central Iran Basins. Geological Society, London, Special Publications. Geological Society, London, 312, pp. 189–203. https://doi.org/10.1144/sp312.9

Garzanti, E., Vermeesch, P., Ando, S., Vezzoli, G., Valagussa, M., Allen, K., Kadi, K.A. and Aljubouy, A.L.A., 2013. Provenance and recycling of Arabian desert sand. Earth-Science Reviews, 120, 1–19. http://dx.doi.org/10.1016/j.earscirev.2013.01.005

Garzanti, E. and Resentini, A., 2016. Provenance control on chemical indices of weathering (Taiwan river sands). Sedimentary Geology, 336, 81–95. http://dx.doi.org/10.1016/j.sedgeo.2015.06.013

Ghasemi-Nejad, A., Asadi, A., Shahmoradi, M., Aghanabati, S.A. and Mohtat T., 2013. Palynostratigraphy and reconsideration of the Shemshak Group in north Isfahan (Kashan–Zefreh) based on dinoflagellate cysts. Scientific Quarterly Journal Geosciences, 86, 99–106. (in Persian with English abstract)

Ghazi, S. and Mountney, N.P., 2011. Petrography and provenance of the early Permian fluvial Warchha Sandstone, Salt Range, Pakistan. Sedimentary Geology, 233, 88–110. https://doi.org/10.1016/j.sedgeo.2010.10.013

Grantham, J.H. and Velbel, M.A., 1988. The influence of climate and topography on rock-fragment abundance in modern fluvial sands of the southern Blue Ridge Mountains, North Carolina. Journal of Sedimentary Petrology, 58, 219–227.

Hayashi, K., Fujisawa, H., Holland, H.D. and Ohmoto, H., 1997. Geochemistry of ~1.9 Ga sedimentary rocks from northeastern Labrador, Canada. Geochimica et Cosmochimica Acta, 61, 4115–4137. https://doi.org/10.1016/S0016-7037(97)00214-7

Herron, M.M., 1988. Geochemical classification of terrigenous sands and shales from core or log data. Journal of Sedimentaty Petrology, 58, 820–829.

Ingersoll, R.V., Fullard, T.F., Ford, R.L., Grimm, J.P., Pickle, J.D. and Sares, S.W., 1984. The effect of grain size on detrital modes; a test of the Gazzi-Dickinson point-counting method. Journal of Sedimentary Petrology, 54, 103–116.

Ingersoll, R.V. and Suczek, C.A., 1979. Petrology and provenance of Neogene sand from Nicobar and Bengal fans. DSDP sites 211 and 218. Journal of Sedimentary Petrology, 49, 1217–1228. https://doi.org/10.1306/212f83b9-2b24-11d7-8648000102c1865d

Iqbal, S., Akhter, G. and Bibi, S., 2015a. Structural model of the Balkassar area, Potwar Plateau, Pakistan. International Journal of Earth Sciences, 104/8, 2253–2272. https://doi.org/10.1007/s00531-015-1180-4

Iqbal, S., Jan, I.U., Akhter, M.G. and Bibi, M., 2015b. Palaeoenvironmental and sequence stratigraphic analyses of the Jurassic Datta Formation, Salt Range, Pakistan. Journal of Earth System Science, 124/4, 747–766. https://doi.org/10.1007/s12040-015-0572-y

Iqbal, S., Wagreich, M., Jan, I.U., Kuerschner, W.M., Gier, S. and Bibi, M., 2019. Hot-house climate during the Triassic/Jurassic transition: The evidence of climate change from the southern hemisphere (Salt Range, Pakistan). Global and Planetary Change, 172, 15–32. https://doi.org/10.1016/j.gloplacha.2018.09.008

Kroonenberg, S.B., 1994. Effects of provenance, sorting and weathering on the geochemistry of fluvial sands from different tectonic and climatic environments. 29th International Geological Congress, Kyoto, Japan, 69–81 pp.

Lee, Y. I., 2002. Provenance derived from the geochemistry of late Paleozoic–early Mesozoic mudrocks of the Pyeongan Supergroup, Korea. Sedimentary Geology, 149, 219–235. https://doi.org/10.1016/S0037-0738(01)00174-9

Mannani, M. and Yazdi, M., 2009. Late Triassic and Early Cretaceous sedimentary sequences of the northern Isfahan Province (Central Iran). Stratigraphy and paleoenvironments. Boleetin De La Socieded Geologica Mexicana, 61, 367–374.

McLennan, S.M., 2001. Relationships between the trace element composition of sedimentary rocks and upper continental crust. Geochemistry, Geophysics, Geosystems, 2/4. https://doi.org/10.1029/2000GC000109

McLennan, S.M., Hemming, S., McDaniel, D.K. and Hanson, G. N., 1993. Geochemical approaches to sedimentation, provenance, and tectonics. In: Johnsson, M.J., and Basu, A. (eds.), Processes Controlling the Composition of Clastic Sediments. Geological Society of America Special Paper, 284, pp. 21–40. https://doi.org/10.1130/SPE284-p21

Nehyba, S., Roetzel, R. and Mastera, L., 2012. Provenance analysis of the Permo-Carboniferous fluvial sandstones of the southern part of the Boskovice Basin and the Zöbing Area (Czech Republic, Austria): implications for paleogeographical reconstructions of the post-Variscan collapse basins. Geologica Carpathica, 63, 365–382. https://doi.org/10.2478/v10096-012-0029-z

Nehyba, S. and Roetzel, R., 2015. Depositional environment and provenance analyses of the Zöbing Formation (Upper Carboniferous–Lower Permian), Austria. Austrian Journal of Earth Sciences, 108/2, 245–276.

Nesbitt, H.W. and Young, G.M., 1982. Early Proterozoic climates and plate motions inferred from major element chemistry of lutites. Nature, 199, 715–717. https://doi.org/10.1038/ 299715a0.

North, C.P., Hole, M.J. and Jones, D.G., 2005. Geochemical correlation in deltaic successions. a reality check. Geological Society of America, Bulletin, 117, 620–632. https://doi.org/10.1130/B25436.1

Nützel, A., Mannani, M., Senowbari-Daryan, B. and Yazdi, M., 2010. Gastropods from the Late Triassic

Nayband Formation (Iran), their relationships to other Tethyan faunas and remarks on the Triassic gastropods body size problem. Neues Jahrbuch für Geologie und Paläontologie, Abhandlungen, 256, 213–228. https://doi.org/10.1127/0077-7749/2010/0049

Pettijohn, F. J., Potter, P. E. and Siever, R., 1987. Sand and Sandstone, 2nd Ed. Springer, 553 pp.

Potter, P.E., Maynard, J.B. and Depetris, P.J., 2005. Mud and Mudstone. Introduction and Overview. Springer, Heidelbeerg, 297 pp.

Roser, B.P. and Korsch, R.J., 1988. Provenance signatures of sandstone-mudstone suites determined using discriminant function analysis of major-element data. Chemical Geology, 67, 119–139. https://doi.org/10.1016/0009-2541(88)90010-1

Sajjadi, F., Hashemi, H. and Borzuee, E., 2015. Palynostratigraphy of the Nayband Formation, Tabas, Central Iran Basin: Paleogeographical and paleoecological implications. Journal of Asian Earth Sciences, 111, 553–567. https://doi.org/10.1016/j.jseaes.2015.05.030

Salehi, M.A., Moussavi-Harami, S.R., Mahboubi, A., Wilmsen, M. and Heubeck, C., 2014. Tectonic and palaeogeographic implications of compositional variations within the siliciclastic Ab-Haji Formation (Lower Jurassic, east Central Iran). Neues Jahrbuch für Geologie und Paläontologie, Abhandlungen, 271/1, 21–48. https://doi.org/10.1127/0077-7749/2014/0373

Salehi, M.A., Mazroei Sebdani, Z., Pakzad, H.R., Bahrami, A., Fürsich, F.T. and Heubeck, C., 2018a. Provenance and palaeogeography of uppermost Triassic and Lower Cretaceous terrigenous rocks of central Iran: Reflection of the Cimmerian events. Neues Jahrbuch für Geologie und Paläontologie, Abhandlungen, 288/1, 49–77. https://doi.org/ 10.1127/njgpa/2018/0723

Salehi, M.A., Moussavi-Harami, R., Mahboubi, A., Fürsich, F.T., Wilmsen, M. and Heubeck, C., 2018b. A tectono-stratigraphic record of an extensional basin: the Lower Jurassic Ab-Haji Formation of east-central Iran. Swiss Journal of Geosciences, 111/1, 51–78. https://doi.org/10.1007/s00015-017-0283-2

Schäfer, P., Senowbari-Daryan, B. and Hamedani, A., 2003. Stenolaemate Bryozoans from the Upper Triassic (Norian–Rhaetian) Nayband Formation, Central Iran. Facies, 46, 135–150. https://doi.org/10.1007/bf02667536

Senowbari-Daryan, B., Rashidi, K. and Beitollah, H., 2011. Hypercalcified sponges from a small reef within the Norian–Rhaetian Nayband Formation near Yazd, central Iran. Rivista Italiana di Paleontologia e Stratigrafia, 117/2, 1–13. https://doi.org/10.13130/2039-4942/5974

Seyed-Emami, K., 2003. Triassic in Iran. Facies, 48, 91–106.

Suttner, L.J., Basu, A. and Mack, G.H., 1981. Climate and the origin of quartzarenite. Journal of Sedimentary Petrology, 51, 1235–1246.

Suttner, L.J. and Dutta, P.K., 1986. Alluvial sandstone composition and paleoclimate; I. Framework mineralogy. Journal of Sedimentary Petrology, 56/3, 329–345.

Taylor, S.R. and McLennan, S.M., 1985. The Continental Crust: Its Composition and Evolution. Blackwell Scientific Publications, 312 pp. http://dx.doi.org/10.1017/S001675680003216

Tortosa, A., Palomares, M. and Arribas, J., 1991. Quartz grain types in Holocene deposits from the Spanish Central System: some problems in provenance analysis. In: A.C. Morton, S.P. Todd, and P.D.W. Huaghton (eds.), Development in Sedimentary Provenance Studies. Geological Society, London, Special Publications. Geological Society, London, 57, pp. 47–54. https://doi.org/10.1144/GSL.SP.1991.057.01.05

Weltje, G. J., Meij, X. D. and De Boer, P. L., 1998. Straitigraphic inversion of siliciclastic basin fills: a note on the distinction between supply signals resulting from tectono and climatic forcing. Basin Research, 10, 129–153. http://dx.doi.org/10.1046/j.1365-2117.1998.00057.x

Wilmsen, M., Fürsich, F.T., Seyed-Emami, K., Majidifard, M.R. and Taheri, J., 2009a. The Cimmerian Orogeny in northern Iran: tectono-stratigraphic evidence from the foreland. Terra Nova, 21, 211–218. https://doi.org/10.1111/j.1365-3121.2009.00876.x

Wilmsen, M., Fürsich, F.T., Seyed-Emami, K. and Majidifard, M.R., 2009b. An overview of the stratigraphy and facies development of the Jurassic System on the Tabas Block, east-central Iran. In: M.-F. Brunet, J.W. Granath and M. Wilmsen (eds.), South Caspian to Central Iran Basins. Geological Society, London, Special Publications. Geological Society, London, 312, pp. 323–343. https://doi.org/10.1144/SP312.15

Wilmsen, M., Fürsich, F., Seyed-Emami, K., Majidifard, M. and Zamani-Pedram, M., 2010. Facies analysis of a large-scale Jurassic shelf-lagoon: the Kamar-e-Mehdi Formation of east-central Iran. Facies, 56, 59–87. http://dx.doi.org/10.1007/s10347-009-0190-8

Yerino, L.N. and Maynard J.B., 1984. Petrography of modern marine sand from the Peru-Chile Trench and adjacent areas. Sedimentology, 31, 83–89. https://doi.org/10.1111/j.1365-3091.1984.tb00724.x

Zahedi, M., 1973. Etude Geologique de la region de Soh (W de l'Iran Central). Geological Survey of Iran, Tehran, 197 pp.

Zimmermann, U. and Spalletti, L.A., 2009. Provenance of the Lower Paleozoic Balcarce Formation (Tandilia System, Buenos Aires Province, Argentina). Implications for palaeogeographic reconstructions of SW Gondwana. Sedimentary Geology, 219, 7–23. http://dx.doi.org/10.1016/j.sedgeo.2009.02.002

Asghar ETESAMPOUR[1], Asadollah MAHBOUBI[1][*],
Reza MOUSSAVI-HARAMI[1], Naser ARZANI[2] & Mohammad
Ali SALEHI[3]

[1] Department of Geology, Faculty of Sciences, Ferdowsi University of
Mashhad, Mashhad, Iran;

[2] Department of Geology, Payame Noor University of Isfahan, Isfahan,
Iran;

[3] Department of Geology, Faculty of Sciences, University of Isfahan, Is-
fahan, Iran;

[*] Corresponding author: mahboubi@um.ac.ir